SSD

SCIENCE FOR A SUSTAINABLE DEVELOPMENT

# DEVELOPMENT OF A NEW LOW-COST AND REGENERABLE DETECTION DEVICE FOR MICROBIAL COMPOUNDS

## MIC-ATR

A. VAN CAUWENBERGE, M. VOUÉ, O. DENIS

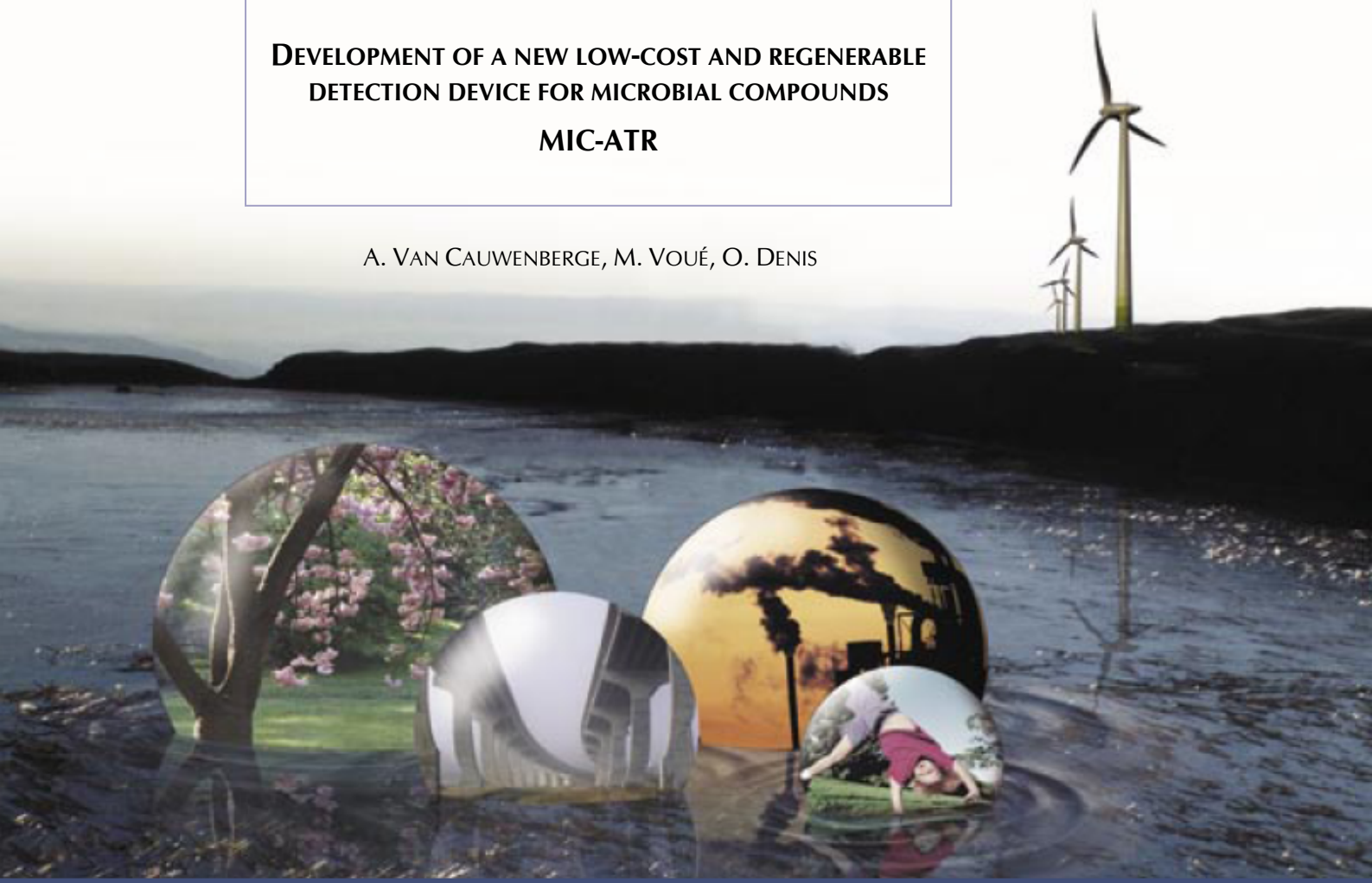

ENERGY

TRANSPORT AND MOBILITY

AGRO-FOOD

HEALTH AND ENVIRONMENT

CLIMATE

BIODIVERSITY

ATMOSPHERE AND TERRESTRIAL AND MARINE ECOSYSTEMS

TRANSVERSAL ACTIONS

.be

**SCIENCE FOR A SUSTAINABLE DEVELOPMENT**
**(SSD)**

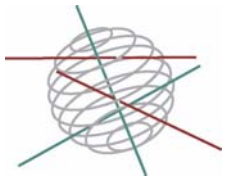

***Health & Environment***

FINAL REPORT PHASE 1

# DEVELOPMENT OF A NEW LOW-COST AND REGENERABLE DETECTION DEVICE FOR MICROBIAL COMPOUNDS

## MIC-ATR

**SD/HE/04A**


**Promotors**

**Dr. E. Noel & Dr. A. Van Cauwenberge**
Hainaut Vigilance Sanitaire (Hygiène Publique en Hainaut)
Boulevard Sainctelette, 55
B-7000 MONS

**Prof. J. De Coninck & Prof. M. Voué**
Université de Mons
Centre de Recherche en Modélisation Moléculaire
Place du Parc, 20
B-7000 MONS

**Dr. K. Huygen & Dr. O. Denis**
ISP-WIV
Département Institut Pasteur de Bruxelles
Unité d'Allergologie
Engelandstraat, 642
1180 BRUXELLES

**Authors**

**A. Van Cauwenberge**
**M. Voué**
**O. Denis**



Rue de la Science 8
Wetenschapsstraat 8
B-1000 Brussels
Belgium
Tel: +32 (0)2 238 34 11 – Fax: +32 (0)2 230 59 12
http://www.belspo.be

Contact person: Emmanuèle Bouregois
+32 (0)2 238 34.94



A. Van Cauwenberge, M. Voué, O. Denis "***Development of a new low-cost and regenerable detection device for microbial compounds MIC-ATR"*** Final Report Phase 1 Brussels : Belgian Science Policy 2009 – 71 p. (Research Programme Science for a Sustainable Development)

## Table of content

## ACRONYMS, ABBREVIATIONS AND UNITS

AFLA-B1: Aflatoxin B1

AFLA-ALB: Aflatoxin B1 coupled to albumin

ATR : Attenuated Total Reflexion

BIA-ATR : Biological Interaction Analysis using Attenuated Total Reflexion

BSA : Bovine Serum Albumin

DNP : 2,4-DiNitroPhenol

DNP-ALB : 2,4-DiNitroPhenol coupled to albumin (equiv. to DNP-HSA)

ELISA: Enzyme Linked ImmunoSorbent Assay

FTIR : Fourier-Transform Infra-Red

HSA : Human Serum Albumin

KLH: Keyhole Limpet Hemocyanin

LPS : LipoPolySaccharides

MoAb: Monoclonal Antibody

NHS : N-hydroxysuccinimidyl

OTS : OctadecylTrichloroSilane

OVA: Ovalbumin

PBS : Phosphate-Buffered Saline

## SUMMARY

There is crucial concern about the presence of molds in indoor environments and their adverse effects on human health. The indoor molds, omnipresent in 60% of the dwellings, have indeed the potential to produce components that have been associated to several severe human health problems like allergic hypersensitivity responses, symptoms of asthma, pulmonary haemorrhage, potentially mortal. For instance, in Belgium, according to the Scientific Institute of Public Health, the prevalence for asthma is about 4% in the global population and is relatively stable between 2001 and 2004.

Fungal spores are universal atmospheric components and are recognized as important causes of respiratory allergies. Fungi grow on most substrates if enough moisture is available, frequently colonize indoor damp places and their spores are commonly found in house dust. More than 80 genera of fungi have been associated with symptoms of respiratory allergy. Among the various mold species Alternaria, Cladosporium, Penicillium and Aspergillus are frequently considered to be important causes of allergic rhinitis.

Four fungal components have been identified as components of interest: VOCs, fungal spores, airborne mycelium fragments, mainly containing glycan wall fragments and mycotoxins, which are non - or weakly volatile stable secondary metabolites.

The links between the presence in the environment of these compounds of interest and identified and declared pathologies is, most of the time, indirect. Among the identified causes of asthma, living in poor indoor environment has often been highlighted. In such kind of environment, dampness is the principal factor of development of mold. Visual inspection doesn't allow to fully asses any adverse health effect. The risk associated to mold should be characterised by the presence of mycotoxins in ambient air. The indoor molds have indeed the potential to produce extremely dangerous toxins. Exposure to these factors has been associated to the several severe human health problems cited above. The most dangerous mycotoxins responsible for these belong to the family of aflatoxins and trichothecenes.

Mycotoxins have been intensively studied in the context of food safety. Mycotoxins, by-products of fungal metabolism, have been implicated as causative agents of adverse health effects in humans and animals that have consumed fungus-infected agricultural products. In this context, the link between the amount of toxin and the observed pathology is more direct. In such a way, normalization actions were carried out, defining the upper admitted levels of such compounds in foodstuffs. These limits are not defined for airborne mycotoxins, due to the lack of experimental data and the absence of reliable sampling and testing procedures.

To date, studies have mostly focused on detecting mycotoxins on bulk materials or in settle dust but there is an urgent need, driven by the guidelines of Public Health policy, to develop specific and sensitive tests to measure airborne macrocyclic trichothecenes mycotoxins in indoor environments, for which no specific nor enough sensitive detection method exists.

Therefore, we propose to overcome these drawbacks by developing a regenerable low-cost biosensor of high sensitivity and selectivity based on FTIR/ATR spectroscopy and to use it to monitor the ligand/receptor interactions of these molecules. The biosen-

sor uses optical elements, transparent in the IR spectral domain, modified by wet chemistry to allow the coupling of molecular receptors.

A Nicolet 380 FTIR spectrometer has been successfully installed at HVS location. The FTIR-sensor experimental cell consists in a vertical ATR SPECAC flow cell connected to a Watson-Marlow peristaltic pump achieving flow rates from 5 to 50 µl/min. The FTIR elements are trapezoidal germanium crystals (50 x 20 x 2 mm³, angle: 45°) that are polished and functionalized at the CRMM. The system has been successfully qualified with two types of FTIR experiments, the determination of the percentage of ethanol in water solutions and the binding of biotin on avidin FTIR sensor.
The equipment was then able to produce experimental results on more sophisticated systems, as we showed with the detection of low molecular weight molecule like DNP which serves as model for detection of haptens. Results obtained by "classical" competitive ELISA and by FTIR were compared, with the use of 6 different rat monoclonal antibodies specific for the DNP. All the tested antibodies responded in a similar manner to the coupled DNP molecules (DNP-HSA) but significant differences were observed for the recognition of free DNP molecules. With coupled DNP molecules, the limits of detection were equivalent between both techniques: in the range of 5-15 ng/ml for the FTIR assays and about 40 ng/ml for the ELISA method, but for the free DNP molecules, the limits of detection were different: 1 µg/ml with ELISA and 4 ng/ml with the FTIR assays using the LO-DNP34 antibody, which is a level comparable to the one obtained with coupled molecules.

The workpackage 2 was dedicated to the detection of aflatoxin B1. Preliminary experiments were run to monitor the binding of an anti-aflatoxin B1 antibody on a functionalized germanium crystal. The molecular layers are equivalent to what has been used for DNP detection. Using a competitive ELISA we tried to determine the concentrations of aflatoxin B1 in our environmental samples. We analysed 36 environmental samples from our collection; 15 of these were previously found to be positive in mass spectometry for the presence of aflatoxin B1. Due to the lower sensitivity of our ELISA assay as compared to the mass spectometry, we were unable to confirm the presence of the toxin in our samples. It should be noted that this lack of sensitivity of optical methods such as ELISA tests can be partially compensated by an appropriated choice of a spectral method for which a dedicated spectral range can be selected to monitor a specific binding. Further experiment to detect the toxin will be carried out during phase 2 of the project.
As molds are very common outdoor but are also present indoor in damp places, quantification of the mold biomass in the ambient air turned out to be interesting in order to better appreciate the level of indoor pollution. Therefore, an additional workpackage has been added, in order to produce and characterise monoclonal antibodies against Alternaria, Aspergillus and Stachybotrys spore fragments.
In order to obtain rat MoAb directed against components of the mold, LOU/c rats were immunized in the foodpats with $5.10^6$ spores of Alternaria alternata (IHEM 18586) or Aspergillus fumigatus (IHEM 6117) or Stachybotrys chartratum (IHEM 22013). At the end of the immunization, lymphocytes were obtained from the poplietal lymph nodes. Lymphocytes were fused with the IR-983F cells. Growing hybridomas were selected in HAT medium. Positive clones were selected by fluorocytometry on various mold spores. Five MoAb were selected from the rats immunized with Alternaria alternata and characterised. LO-ALT-3 was shown to be clearly species specific while LO-ALT 5 seems very interesting to detect a large array of mould species in environmental

samples. We analysed the ability of LO-ALT-5 MOAb to detect the antigen in environmental samples, coming from dust vacuumed on one hundred centimetres square surface from ten different living rooms. The ELISA with LO-ALT-5 was able to detect the presence of an antigen in four out of ten samples. Six other MoAbs have been selected from rats immunized with Aspergillus. From these six antibodies LO-ASP-2 demonstrated a very good binding on Aspergillus niger spores and a low binding to Alternaria, Cladosporium and Stachybotrys spores. Five others MoAbs have been obtained from rats immunized with Stachybotrys. These antibodies need to be better characterized before being used in our biosensor.
The anti-Alternaria MoAbs were successfully immobilized at the surface of the optical sensor and their spectral response monitored, as a function of the dilution of the Alternaria extract, in the polysaccharide and in the protein spectral domains. Preliminary results show that the antibodies mainly respond to the polysaccharide part of the antigen.

The workpackage 3 was dedicated to the production of monoclonal antibodies against mycotoxins. As mycotoxins are small non proteinic components, they are not able to induce the production of antibodies when injected "as this" in animals since the production of antibodies (at least for non repetitive antigens) requires the help of T helper cells recognizing linear peptides. Indeed the activation of B cells, their production of antibodies and the generation of MoAb upon immunization requires the conjugation of the toxins to carrier proteins.

Therefore Roridin A and Verrucarin A were conjugated to the KLH and OVA. Since these toxins do not have a functional group to facilitate their conjugations, they were treated with succinic anyhydride to generate bis-hemisuccinate. An activated N-hydroxysuccinimide intermediate of the toxins-hemisuccinate was synthesized. Protein toxins conjugates were then prepared by coupling the activated ester reactive intermediate to the carrier's proteins using N,N′-Dicyclohexylcarbodiimide.
LOU/c rats were immunized in the foodpats with 50 µg of roridin A or verrucarin A conjugated to the KLH. At the end of the immunizations, lymphocytes were obtained from the poplietal lymph nodes. Lymphocytes were fused with the IR-983F cells. Growing hybridomas were selected in HAT medium.

The efficiency of the immunization/fusion was confirmed by the presence of numerous clones specific for the KLH. More than 300 clones have been obtained and analysed. More than 60% of these clones were specific for the KLH but none were directed against the mycotoxins.

Therefore we decided to use another coupling reaction. We still generated a bis-hemisuccinate of the roridin A or the verrucarin A and these products were immediately coupled to the proteins (BSA, OVA or KLH) using a water soluble carbodiimide (1-ethyl-3-(3-dimethylaminopropyl)carbodiimide hydrochloride).
LOU/c rats were immunized in the foodpats with 50 µg of verrucarin A conjugated to the BSA. Poplietal lymph node cells were fused to IR-983F cells. Growing hybridomas were selected in HAT medium and their supernatants were tested by ELISA on plated coated with BSA (to monitor for the secretion of antibodies specific to the carrier) or plates coated with BSA-Verrucarin A to detect mycotoxin specific antibodies.
Eight different MoAb recognizing the mycotoxins were obtained. Supernatants from some of these clones contained antibodies recognizing verrucarin A in the context of different carriers (BSA, OVA and KLH). Some antibodies were also cross-reactive

against the roridin A. We investigated the fine specificities of these MoAb but the results indicated that our antibodies were only detecting the coupled toxin (in a proteinic context) but not the free toxin, therefore impending further development of our detection assays. Therefore we started new fusion experiments with LOU/c rats immunized in the foodpats with 50 µg of verrucarin A conjugated BSA. Poplietal lymph node cells were fused to IR-983F cells. Growing hybridomas were selected in HAT medium and their supernatants were tested by ELISA on plated coated with OVA-Verrucarin A in the absence or in the presence of 10 µg/ml of free verrucarin A (to directly monitor the binding of antibodies to the free verrucarin A). Of the 553 tested clones, 70 clones (13%) produced antibodies recognizing the verrucarin A bound to OVA. Only one of these clones produced antibodies which were inhibited by the free verrucarin A. After optimization of a competitive ELISA test using this antibody (F24-1G2), we obtained sensitivity between 3.9 and 1.9 ng/ml of free verrucarin A. In the next step we will use this assay in order to detect the verrucarin A in our environmental samples.

About 40 samplings were carried out in contaminated houses during the first semester 2008. The airborne toxins were collected on quartz filters (pore diameter: 2.2 µm) by sucking an air volume corresponding to that of ½ of the space at a flow rate of 400 L/min. In parallel to the development of our analytical tools, a cross-validation was requested at the University of Ghent (Prof. S. De Saeger) who analyzed the samples by LC-MS-MS.
In 15 of these 40 samples, mycotoxins were readily detected as concentration statistically significant. Unexpectedly, Aflatoxin B1 was also found, shedding a new light on WP2, which becomes for these reasons of great importance.
A comparison was also carried out with the commercial ELISA test Envirologix®. Discrepancies between LC-MS-MS results and ELISA results are important and the former seems to systematically under-evaluate the contamination.
Concomitantly, about 40 samples were also collected in non-contaminated houses ("blank"), following the sampling procedure previously described, in order to make comparisons and build the first step of an epidemiologic study campaign that could be carried out in a forthcoming project.

In conclusion, the **technology transfer** between UMons and HVS successfully occurred. On the **DNP model system**, an inhibition optimized ELISA test has been set-up, with a comparison between free DNP and DNP coupled to albumin. Immuno-assays concepts have been successfully transferred to FTIR sensors domain, yielding a new sensors category: FTIR immuno-sensors. **Monoclonal antibodies against Alternaria, Aspergillus and Stachybotrys were produced and partially characterized.** In particular, we have developed and characterized two antibodies (LO-ALT-1 and LO-ALT-5) specific for an antigen present at the surface of mould spores and another antibody (LO-ALT-3) recognizing an antigen specific for Alternaria alternata. We have started to produce and purify these antibodies in order to use them in our biosensor device to quantify the mould biomass indoor. **The production of MoAbs against mycotoxins is ongoing.** Five cross-reactive rats MoAb are recognizing both the roridin A and the verrucarin A but one antibody, the F24-1G2 allows the detection of free verrucarin A with a sensitivity between 3.9 and 1.9 ng/ml.
**Environmental sampling started Jan. 2008 and is still ongoing.** Cross-validation has been carried out with LC-MS-MS technique, as well as with ELISA (Envirologix®). The latter technique seems to systematically under-evaluated the contamination level.

# 1. INTRODUCTION

## 1.1 Context

Recent research in Health (in particular, the increased prevalence of allergy) has substantially increased the awareness of the importance of healthy and safe housing conditions.

The US CDC (Centre for Disease Control and Prevention) has shown between 1980 and 1994 an increased prevalence of asthma in the U.S. of 75 % in the overall population and of 74% among children 5-14 years of age. Therefore asthma is a major chronic illness accounting for more than 10 million outpatient clinic visits, and nearly 2 million emergency visits each year. According to the National Heart, Lung and Blood Institute 2002 Chartbook, annual expenditure for health and lost productivity due to asthma were $ 14 billion in 2002.

In Belgium, according to the Scientific Institute of Public Health, the prevalence for asthma is about 4% in the global population and is relatively stable between 2001 and 2004. In the province of Hainaut, the situation is statistically difference and the prevalence reaches levels around 6.0, as shown in **Figure 1**.

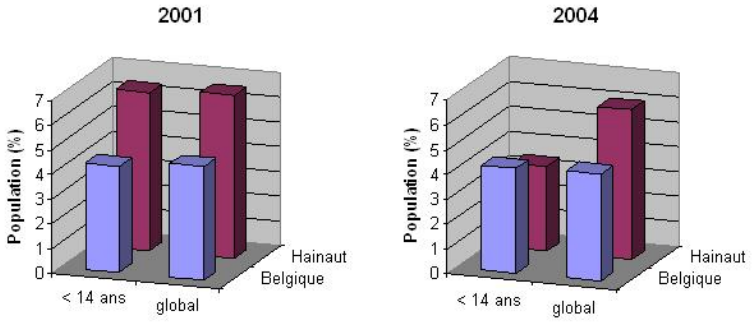


**Figure 1** : Asthma prevalence in Belgium for years 2001 and 2004 (data source: SIPH, Brussels)

Fungal spores are universal atmospheric components and are recognized as important causes of respiratory allergies. Fungi grow on most substrates if enough moisture is available, frequently colonize indoor damp places and their spores are commonly found in house dust. More than 80 genera of fungi have been associated with symptoms of respiratory allergy. Among the various mold species Alternaria, Cladosporium, penicillium and aspergillus are frequently considered to be important causes of both allergic rhinitis.

Moreover, recent studies (link to the reference) whose results are summarized by Prof. F. Squinazi, Head of the Laboratoire d'Hygiène de la Ville de Paris, point out the following sticking features :

- In Europe and North America, molds are present in 20% to 40% of the buildings
- A study carried out in France over the period 2003-2007 over 567 buildings highlighted that 47% of them encountered problems that could be directly related to ambient humidity
- In USA, 20% to 30% of atopic patients are concerned by the allergy to indoor molds, which corresponds to 6% of the total population.

**Figure 2** : Contaminated buildings (Source: Laboratoire de prévention des Pollutions Interieures (LPI), HVS, Mons, Belgium)

In these studies, four fungal components have been identified as components of interest :

- The organic volatile compounds (OVCs)
- The fungal spores
- The airborne mycelium fragments, mainly containing glycan wall fragments
- The mycotoxins, which are non- or weakly volatile stable secondary metabolites

The links between the presence in the environment of these compounds of interest and identified and declared pathologies is, most of the time, indirect. Among the identified causes of asthma, living in poor indoor environment has often been highlighted. In such kind of environment, dampness is the principal factor of development of mold. Visual inspection doesn't allow to fully assessing any adverse health effect. The risk associated to mold should be characterised by the presence of mycotoxins in ambient air. The indoor molds have indeed the potential to produce extremely dangerous toxins. Exposure to these factors has been associated to several severe human health problems like allergic hypersensitivity responses, symptoms of asthma, pulmonary haemorrhage, potentially mortal. The most dangerous mycotoxins responsible for these belong to the family of aflatoxins and trichothecenes.

Mycotoxins have been intensively studied in the context of food safety. Mycotoxins, by-products of fungal metabolism, have been implicated as causative agents of adverse health effects in humans and animals that have consumed fungus-infected agricultural products. In this context, the link between the amount of toxin and the observed pathology is more direct. In such a way, normalization actions were carried out, defining the upper admitted levels of such compounds in foodstuffs.

**It should be kept in mind that these limits are not defined for airborne mycotoxins, due to the lack of experimental data and the absence of reliable sampling and testing procedures.**

The fungi are a vast assemblage of living organisms, but mycotoxin production is most commonly associated with the terrestrial filamentous fungi called the molds. Various genera of toxigenic fungi are capable of producing such diverse mycotoxins as the aflatoxins, rubratoxins, ochratoxins, fumonisins, and trichothecenes. The trichothecenes are a very large family of chemically related toxins produced by various species of Fusarium, Myrotecium, Trichoderma, Cephalosporium, Verticimonosporium, and Stachybotrys. They are markedly stable under different environmental conditions. The distinguishing chemical feature of macrocyclic trichothecenes is the presence of a trichothecene ring, which contains an olefinic bond at C-9, 10; and an epoxide group at

C-12,12 .

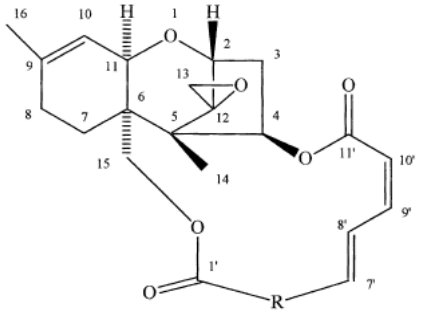

| Compound | R |
|---|---|
| Roridin A (**1**) | —CHOHCH(CH$_3$)CH$_2$CH$_2$OCHCHOHCH$_3$ (*S*) (*R*) (*R*) (*R*) |
| Verrucarin A (**2**) | —CHOHCH(CH$_3$)CH$_2$CH$_2$OC=O (*S*) (*R*) |

**Figure 3 :** Molecular structure of some D-class macrocyclic trichothecenes: Roridin A and Verrucarin A.

## 1.2 Objectives and expected outcomes

### a) Objectives

To date, studies have mostly focused on detecting mycotoxins on bulk materials or in settle dust but there is an urgent need, driven by the guidelines of Public Health policy, to develop specific and sensitive tests to measure airborne macrocyclic trichothecenes mycotoxins in indoor environments, for which no specific nor enough sensitive detection method exists.

**The aim of this research programme is double: the network proposes to develop a regenerable low-cost biosensor of high sensitivity and selectivity based on FTIR/ATR spectroscopy and to use it to monitor the ligand/receptor interactions of these molecules. Additionally, field samples originating from contaminated and non-contaminated houses will be analyzed and, when possible, correlations will be drawn between the microbial compounds levels and epidemiologic variables.**

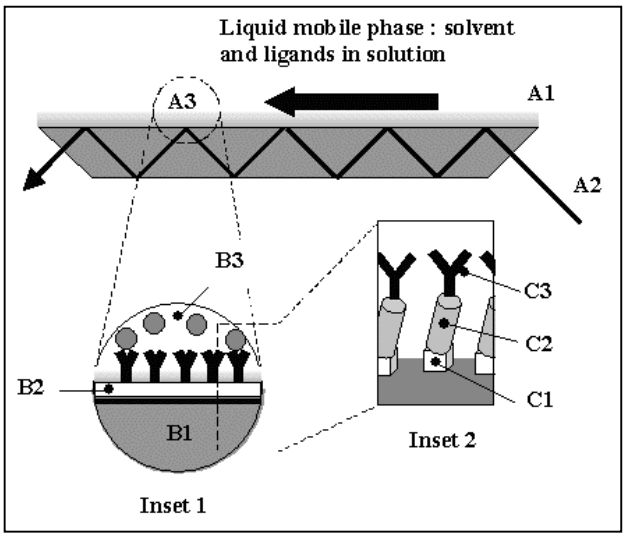


**Figure 4 :** A1: Total internal reflection element transparent in the infra-red spectral domain; A2: Incident infra-red beam; A3: Ligand/receptor interactions at the crystal surface and evanescent wave). Inset 1: Molecular recognition (B1: ATR element surface; B2: Functionalization layer; B3: Free ligands and ligands bound to receptors). Inset 2: Schematic representation of the molecular construction (C1: anchoring molecule; C2: spacer molecule; C3: receptor).

(Voué, M; Goormaghtigh, E., Homble, F.; Marchand-Brynaert, J; Conti, J.; Devouge, S.; De Coninck, J. Langmuir 2007, 23, 949-955.)

The biosensor will use optical elements, transparent in the IR spectral domain, modified by wet chemistry to allow the coupling of molecular receptors, in particular mouse or rat monoclonal antibodies directed against macrocyclic trichothecenes (Figure 4). Trichothecene-specific antibodies will be generated using hybridoma technology and producing clones will be identified, expanded and characterized. Purified antibodies will be used as receptors in the new optical biosensor.

Besides the quantitative determination of the trichothecenes toxins concentration, the research partners will help in the initiation of actions on standardisation and normalisation by defining detection limits and providing reliable sampling methods for indoor environment.

**b) Expected outcomes**

The scientific and technological prospects opened by the **MIC-ATR** project are associated with breakthrough innovations introduced for the first time to achieve a complete characterisation of the trichothecene mycotoxins detection in indoor environments with the purpose of developing a new biosensor technology and of determining its sensitivity limit and performances. These innovations are mainly represented by the development of a new generation, fully characterised, of biosensors capable to provide a cost-effective and reliable method to detect endotoxins and trichothecene mycotoxins.
Fundamental research proposed by the MIC-ATR partners considers highly strategic the development of a conceptual research that is, since the beginning, addressed to develop all standardisation aspects that today affect the comparability of published results. In fact, one major topic for the realisation of these biosensors is to have a standard base. The use of the MIC-ATR system can effectively open a new "standard" for mycotoxins detection.

In particular, **the expected research results and deliverables (D) are the following**. The related WP and the expected delivery times are given in parenthesis on a t0+x months basis.

D0: Revised workprogram and workpackages (Expected at t0 + 3).
D1: Capability of detecting DNP using a functionalized germanium ATR element (related to WP1 – Expected at t0+18).
D2: Capability of binding commercial antibodies against AFLATOXINS (related to WP2 – Expected at t0+18).
D3: Capability of detecting AFLATOXINS using a functionalized germanium ATR element coated with COMMERCIAL ANTIBODIES (related to WP2 – Expected at t0+24).
D4: Dissemination activities related to WP1 and WP2 (scientific publications, …) (Expected between t0+18 and t0+27).
D5: Capability of producing POLYCLONAL ANTIBODIES against MACROCYCLIC trichothecene mycotoxins (related to WP3 – Expected at t0+12).
D6: Capability of producing MONOCLONAL ANTIBODIES against MACROCYCLIC trichothecene mycotoxins (related to WP3 – Expected at t0+18).
D7: Method for ENVIRONMENTAL SAMPLING of TRICHOTHECENES MYCOTOXINS (related to WP3 – Expected at t0+36).
D8: Capability of detecting MYCOTOXINS using a functionalized germanium ATR element coated with ANTIBODIES produced during WP3 (Expected at t0+48).

New deliverables added after revision of work program and workpackages.

D9*: Capability of producing MONOCLONAL ANTIBODIES against SPORE FRAGMENTS (related to new WP – Expected at t0+12).
D10*: Capability of detecting SPORE FRAGMENTS using a functionalized germanium ATR element coated with ANTIBODIES produced during WP3 (related to new WP – Expected at t0+24).
D11*: Dissemination activities related to WP3 (scientific publications, …) (Expected between t0+36 and t0+48).

## 2. COLLABORATION AND SYNERGY WITHIN THE NETWORK

In indoor pollution, studies have mostly focused on detecting mycotoxins on bulk materials or in settle dust but there is an urgent need, driven by the guidelines of Public Health policy, to develop specific and sensitive tests to measure airborne macrocyclic trichothecenes mycotoxins in indoor environments, for which no specific nor enough sensitive detection method exists.

The **MIC-ATR** project proposes to overcome in 4 years these drawbacks in developing a regenerable low-cost biosensor of high sensitivity and selectivity based on FTIR/ATR spectroscopy, and in applying this technology to the selected topics of high interests such as the detection of AFLATOXIN B1, MYCOTOXINS and SPORES fragments.

The links between the research activities inside the Consortium and the expertise of the research partners are described in Figure 5 and Figure 6.

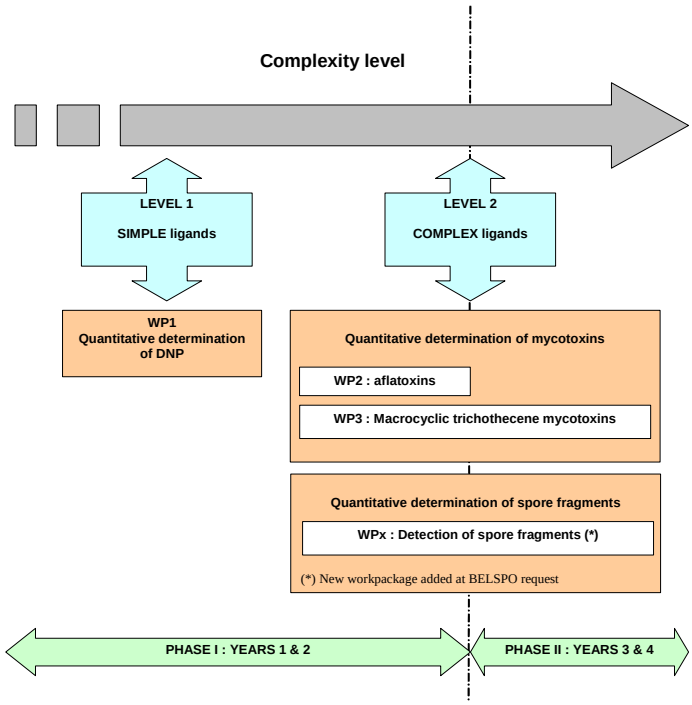


**Figure 5 :** Links between the MIC-ATR research activities.

**To date, the research network is perfectly operating, including researcher exchange between the research units, as well as period project review meetings (at least one per month) to focus to research activities on the hottest topics of the project and keep them in phase with the initial planning.**

Some collaboration has been initiated outside the networks, with partners of the Follow-Up Committee (in particular with Prof. S. De Saeger, Univ. Ghent) in a view of strengthening the scientific basis of the project as well as the issues relevant of the dissemination of the results.

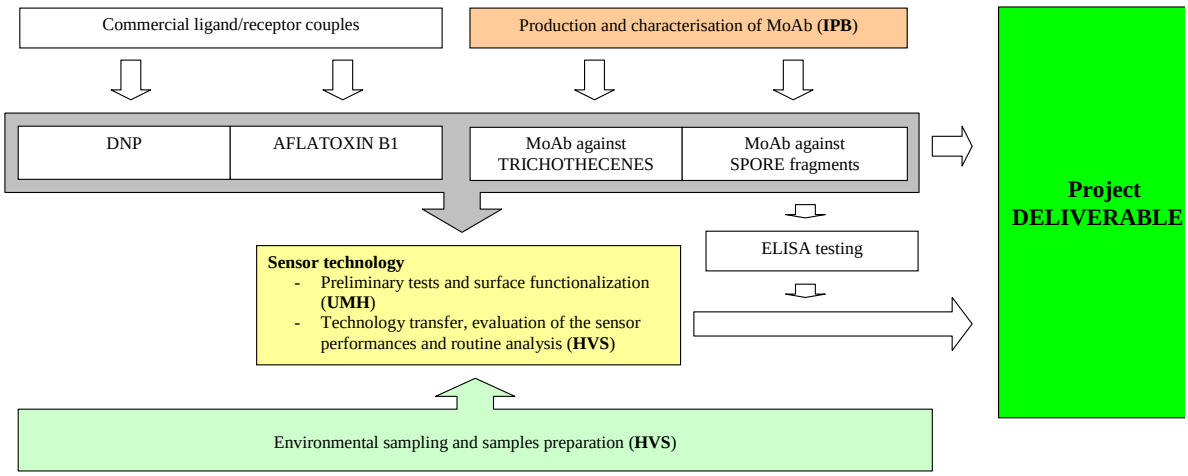


**Figure 6 :** Scientific expertise of the MIC-ATR project partners.

## 3. REPORT OF THE PROGRESS AND IMPLEMENTATION OF THE METHODOLOGY

The results reported hereafter mainly concern the workpackages 1 to 3, as well as qualification of new instruments installed at HVS location (and the technology transfer related to it from UMONS). They have been organized as follows and the related workpackages are given between parentheses :

A) Installation and qualification of new instruments at HVS location
B) DNP detection : ELISA and FTIR analysis (WP1)
C) Detection of AFLATOXIN B1 (WP2)
D) Production and characterisation of monoclonal antibodies against ALTERNARIA, ASPERGILLUS and STACHYBOTRYS spore fragments (Additional WP)
E) Production of monoclonal antibodies against mycotoxins (WP3)
F) Environmental sampling (WP3)

### A. Installation and qualification of new instruments at HVS location.

*a) Environmental sampling systems.*

High flow-rate pumps (RAVEBO SUPPLY B.V) have been installed at HVS located, dedicated to environmental sampling. They allow the sampling to be carried out at a flow rate of 100 to 600 litre/minute (6-36 m³/hour) (Figure 7).

Environmental sampling plans are currently designed. They will be coupled to the standard activities of HVS teams in indoor pollution prevention and diagnosis.

**Figure 7 :** High flow rate pump for environmental sampling

b) FTIR equipment.

A Nicolet 380 FTIR spectrometer has been installed at HVS location. The FTIR-sensor experimental cell consists in a vertical ATR SPECAC flow cell connected to a Watson-Marlow peristaltic pump achieving flow rates from 5 to 50 µl/min (Figure 8).

**Figure 8 :** Nicolet 380 FTIR spectrophotometer with peristaltic pump

The FTIR elements are trapezoidal germanium crystals (50 x 20 x 2 mm³, angle: 45°) that are polished and functionalized at the CRMM. These crystals allow 25 internal reflexions of the FTIR beam to occur, increasing in such a way the sensitivity of the detection.

c) Qualification of new instruments

The new FTIR equipment has been qualified on 2 types of FTIR experiments. The first one is a standard FTIR experiments and concerns the determination of the percentage of ethanol (EtOH) in water solutions. Solutions with EtOH percentage ranging from 0 to 90% have been tested and the FTIR spectra recorded for further analysis. They were processed using a standard multivariate analysis method (PLS) on three spectral regions (Figure 9A) and the results were compared to those obtained on the equipment of the CRMM. No significant statistical difference was observed (Figure 9B)

**( A )** **( B)**

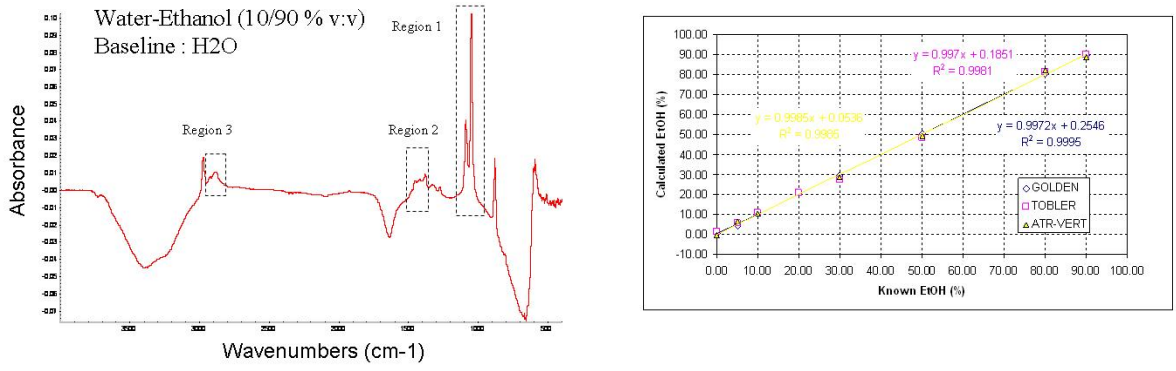


**Figure 9 : (A)** Absorbance spectrum of a 90% ethanol solution in water – Determination of the spectral domains characteristics for the PLS analysis. **(B)** Partial least-squares (PLS) calibration for water/ethanol solutions – Comparison with others instruments (Nicolet 6700) and different experimental flow cells.

The second series of experiments concerns the binding of BIOTIN on AVIDIN FTIR sensor. The sensor was prepared as reported in Voué (2007). Figure 10A shows the progressive binding of the protein, as evidenced by the growth of the intensity of the amide I and II absorption bands and the decrease of the intensity of the $COO^-$ band associated to the spacer molecule (SADP, Pierce).

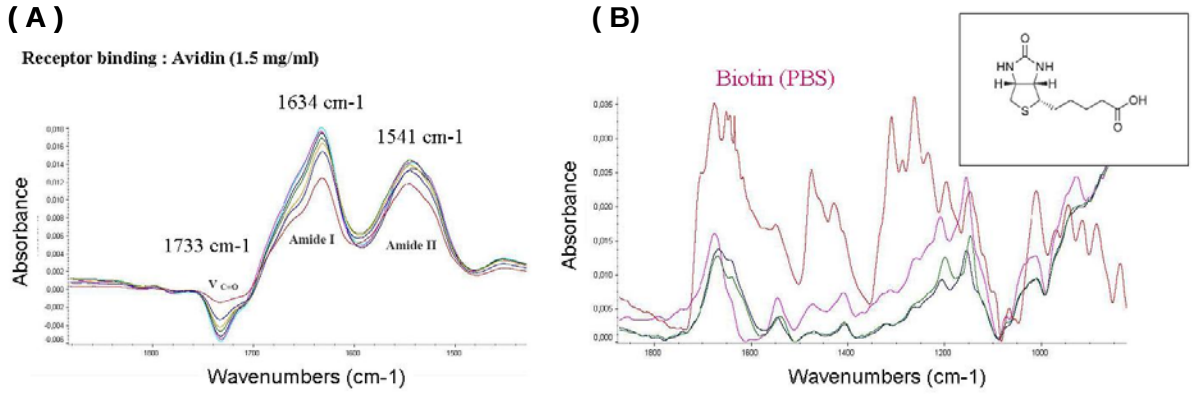


**Figure 10 : (A)** Binding of Avidin to the FTIR sensor surface. **(B)** Binding of biotin to the avidin functionalized FTIR biosensor surface – Comparison between bound biotin spectra and spectrum of free biotin in PBS solutions.

Figure 10B compares the spectra of BIOTIN in PBS solution with spectra obtained for BIOTIN bound the AVIDIN molecules at the level of the FTIR sensor surface. Spectral regions of interest can be adequately identified in such a way. It should be noted that most of these absorption bands are below 1500 $cm^{-1}$ and can not be observed using silicon substrates due to the strong absorption of FTIR radiation below that limit.
On the basis of these two sets of experiments, the new equipment is considered to be validated for the detection applications and is able to produce experimental results comparable to those obtained at the CRMM on more sophisticated systems.

## B. DNP detection: ELISA and FTIR analysis (WP1).

This part of the report concerns the comparative detection of a low molecular weight molecule (DNP) by ELISA and FTIR. The choice of this molecule has been made because it may be considered as an appropriate model for detection of haptens.

### a) ELISA tests results

A "classical" competitive ELISA has been used to detect the free DNP in solution and to determine the detection limit of this technique in these particular conditions. Since the detection limit is clearly dependant of the characteristics of the antibodies used in the assay, we performed this competitive ELISA with six different rat MoAb specific for the DNP. The characteristics of these antibodies (antigen used for rat immunization, isotype and affinities) are listed in Table 1. To detect the DNP, BSA labelled DNP was coated on ELISA plates; then the plates were saturated and washed. Decreasing concentration of inhibitors (free DNP or BSA labelled DNP) was applied together with a fixed concentration (1 µg/ml) of rat MoAb against DNP. After the incubation the plated were washed and the binding of the rat MoAb to the coated BSA-DNP was revealed by a mouse MoAb labelled with the peroxydase and specific for the rat Kappa light chain.

| Name | Antigen | Isotype | Affinity |
|---|---|---|---|
| LO-DNP-1 | DNP-OVA | IgG1 | 8.4 10E10 |
| LO-DNP-2 | DNP-Ascaris | IgG1 | 1.7 10E10 |
| LO-DNP-34 | DNP-OVA | IgM | 5.5 10E10 |
| LO-DNP-45 | DNP-salmonella | IgA | 3.2 10E10 |
| LO-DNP-57 | DNP-salmonella | IgG2b | 1.4 10E10 |
| LO-DNP-61 | DNP-salmonella | IgG2a | 7.1 10E10 |

**Table 1:** Characteristics of the rat antibodies specific for DNP used.

As shown in Figure 11, the binding of the six rat MoAb was inhibited in the same way by the free BSA-DNP in solution leading to an assay sensitivity located between 80 and 40 ng/ml. However only the binding of LO-DNP-2 and -61 showed an inhibition of more than 50% at the highest concentration of DNP tested (1 mg/ml) and this assay showed a very poor sensitivity (between 8 to 4 µg/ml).

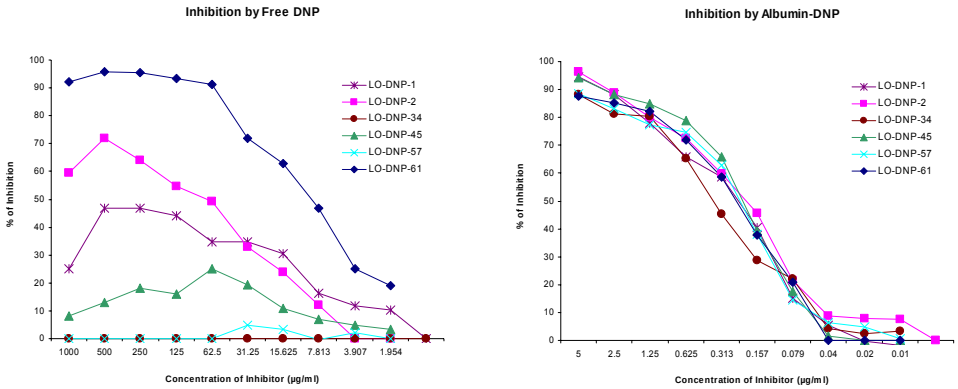


**Figure 11 :** Detection of free DNP or BSA-DNP using six different rat MoAb in a competitive ELISA – Effect of the anti-DNP monoclonal antibodies

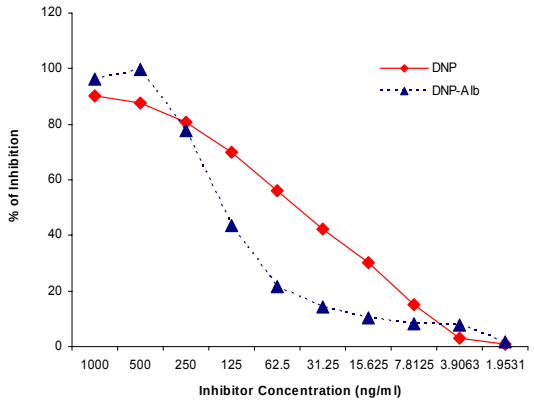


Therefore we worked to optimize the detection of the free DNP in this assay. We optimized the concentrations of BSA-DNP used for the coating, the concentrations of LO-DNP-61 in solution and the duration of the different incubations. This optimized competitive ELISA assay had a 1000 x higher sensitivity for the free DNP and the level of free DNP detection was located between 8 to 4 ng/m l(Figure 12).

**Figure 12 :** Detection of free DNP and of DNP coupled to albumin molecules – Optimization of the competitive ELISA towards an increased sensitivity for the free DNP

b) FTIR analysis results

The optical device for the detection of 2,4-DNP is build on a Germanium crystal covered by an octadecyl-trichlorosilane (OTS) self-assembled monolayer coupled to a spacer molecule whose end function is an N-hydroxysuccynimidyl ester (Figure 13A). Reference spectrum of 2,4-DNP were measured in diluted and concentrated solutions (PBS solution) and compared to spectrum of the SpectraOnline database. Among the peaks reported in Table 2, vibrational peaks with high intensity are identified at 1268, 1346, 1556 and 1607 cm $^{-1}$ and will be followed during the detection experiment.

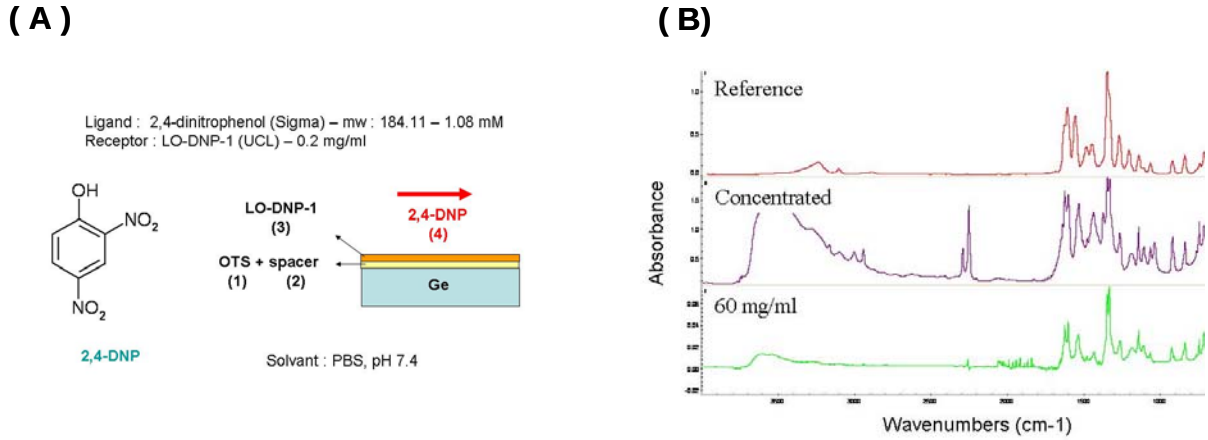


**Figure 13 :** (A) Detection principle for 2,4-DNP using monoclonal antibodies. (B) Reference spectrum of 2,4-DNP – Comparison with DNP spectra in concentrated and diluted (60 mg/ml) solutions.

| Position | Intensity | Position | Intensity |
|---|---|---|---|
| 640.5 | 0.131 | 1346.8 | 1.281 |
| 711.1 | 0.276 | 1447.1 | 0.368 |
| 841.0 | 0.250 | 1483.6 | 0.339 |
| 919.8 | 0.168 | 1556.0 | 0.711 |
| 1065.2 | 0.145 | 1607.1 | 0.819 |
| 1140.5 | 0.243 | 3104.4 | 0.0733 |
| 1204.3 | 0.302 | 3235.8 | 0.148 |
| 1268.7 | 0.485 | | |

**Table 2:** Characteristics vibrational peaks of 2,4-DNP

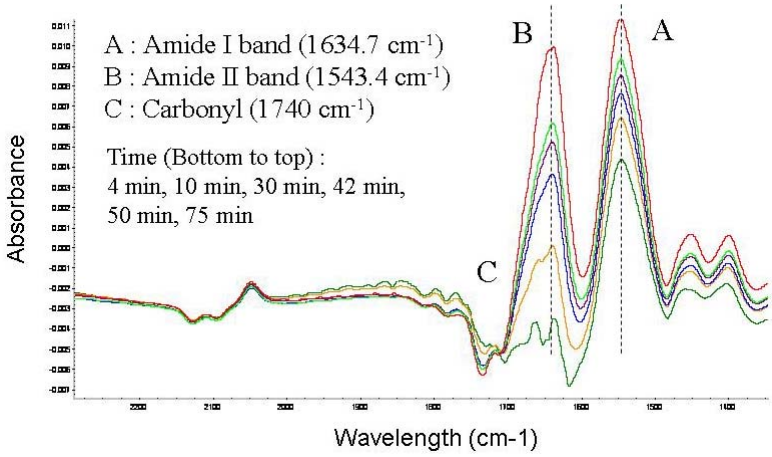


**Figure 14 :** Binding of the LO-DNP1 anti-DNP monoclonal antibody – Time evolution of the amide bands.

As shown on Figure 14, the binding of LO-DNP1 monoclonal antibody against 2,4-DNP is clearly evidenced by the increase of the intensity of the amide I (1634 $cm^{-1}$) and II (1543 $cm^{-1}$), as well as by the decrease of the carbonyl band at 1740 $cm^{-1}$. Similar binding curves were observed for LO-DNP34 and LO-DNP61 antibodies. The MoAb layer was stable under rinsing by a PBS solution.
The second stage of the experiments concerns the detection of the ligand, itself. Solutions of free DNP were flown in the experimental cell but no significant increase of the DNP absorption peaks was observed at 1268, 1346, 1556 and 1607 $cm^{-1}$ (data not shown). An *a posteriori* explanation is given by the poor affinity of the MoAB for free DNP as evidenced by the ELISA results (Figure 12).

Experimental procedure has been reoriented towards the detection of DNP coupled to albumin and towards competition tests. The methodology is therefore the following.

In a first step, a DNP-HSA solution (1 mg/mL in PBS) was injected in the flow cell at a flow rate of 5 to 10 µL/min (discontinuous). After 2 h, buffer solution was injected in the cell to remove the unreacted excess of protein. After the binding of the protein to the sensor surface, monoclonal antibodies (Mabs) (5 µg/mL in PBS) were incubated at room temperature in the presence of either free or coupled DNP. After 20 min of incubation, an aliquot of the Mabs/inhibitor solution was injected in the flow cell and the binding of the antibody to the immobilized protein was monitored as a function of time by recording FTIR spectra.

A series of inhibition tests was carried out to probe the sensitivity of the detection method with respect to the coupled or to the free DNP. After binding the coupled protein to the sensor surface, solutions containing Mabs and inhibitors were injected in the flow cell after 20 min of incubation at room temperature. The absorbance of the sample is easily converted in percentage of inhibition by

$$I = 100\left(1 - \frac{A_i - A_0}{A_{\max} - A_0}\right)$$

where $A_i$ is the absorbance of the sample, $A_0$ is the absorbance measured after the binding of the protein and the subsequent rinsing with PBS and $A_{max}$ the absorbance measured in the absence of inhibitor. In each case, the absorbance refers to the amide II band.

We considered two types of inhibitors: free DNP and DNP-HSA molecules. Using this experimental scheme, three monoclonal antibodies against DNP were tested: LO-DNP61, LO-DNP34 and LO-DNP01. The results presented in Figure 15 clearly show that these antibodies respond in a different manner to the free or to the coupled molecule. The sensitivity is about 10 to 100 times higher for the coupled molecule than for the free antigen (Figure 15A). More interesting is the fact that the response of the test also depends on the antibody for the free antigen, although the responses are equivalent for coupled DNP. In the case of free DNP, the LO-DNP34 has sensitivity about 100 times less than the other types of antibodies. It should also be pointed out that the LO-DNP61 antibodies interact with the free DNP molecules (Figure 15, filled circles) in a way similar to the one they interact with the hapten-carrier complexes, at least at low concentration of inhibitors.
Similar experiments were carried out using ELISA technique. Their results are presented in Figure 15B. The curves are steeper than for the FTIR sensors. All the tested antibodies respond in a similar manner to the coupled DNP molecules (open symbols) but significant differences are observed for the recognition of free DNP molecules (filled symbols). Sensitivity is about 100 times higher for LO-DNP61 but LO-DNP34 does not recognize the free DNP molecules.

For the DNP-HSA inhibitors, the limits of detection are equivalent between both techniques: in the range 5 – 15 ng/mL (FTIR assays) and about 40 ng/mL (ELISA). For the free DNP molecules, the limits of detection are different: higher than 1 µg/mL (ELISA for all the antibodies and FTIR for LO-DNP34) but detection limit of 4 ng/mL was estimated using FTIR assays and LO-DNP61 antibody, which is a level comparable to those estimated for the coupled molecules. Further information is given in the original publication (doi:10.1016/j.bios.2009.01.001 ).

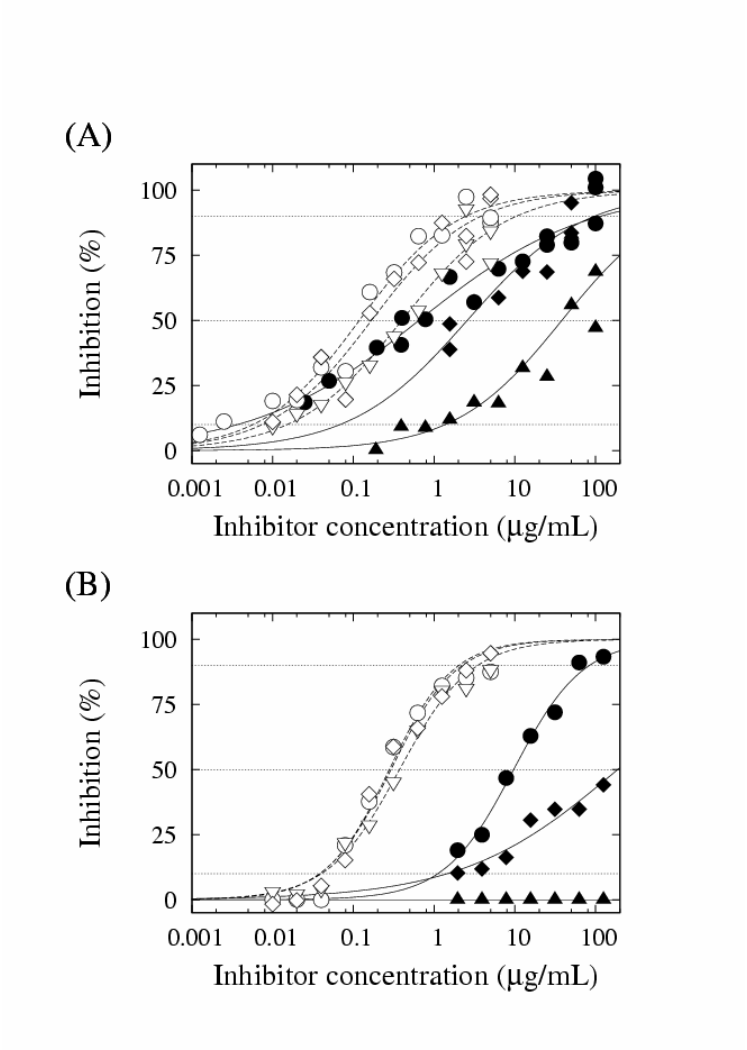


**Figure 15 :** Inhibition curves for DNP-HSA (open symbols) and free DNP (filled symbols) using (A) FTIR immuno-sensors and (B) ELISA – Influence of the antibody (circles: LO-DNP61, triangles: LO-DNP34, diamonds: LO-DNP01).

### C. Detection of AFLATOXIN B1 (WP2)

In this workpackage, preliminary experiments were run to monitor the binding of an anti-aflatoxin B1 antibody on a functionalized germanium crystal. The molecular layers are equivalent to what has been used for DNP detection (Figure 13A).

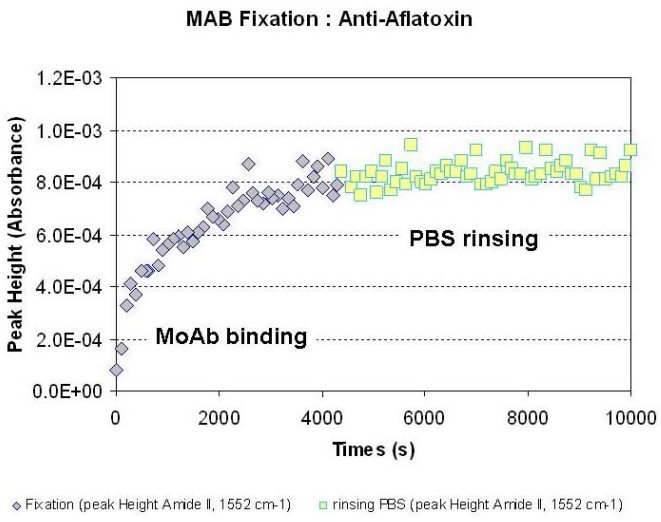


**Figure 16 A :** Binding of the anti-aflatoxin B1 antibody – Time evolution of the amide II bands (1552 $cm^{-1}$).

Binding of the MoAb was investigated over 4000 s and monitored by the intensity of the amide II band. After that time, a PBS solution was flown into the experimental cell, showing that the bound layer was stable (Figure 16 A).
First step of the detection process is achieved. Further experiment to detect the toxin will be carried out during phase 2 of the project.

We have set up a competitive ELISA able to quantify the concentration of aflatoxins in solutions. We used bovine serum albumin labelled with aflatoxin B1 (from Sigma-aldrich) as a coating antigen and clone AT-B1 (mouse monoclonal antibody specific for aflatoxin B1, from Sigma-Aldrich) as detecting antibody. We optimalised the concentrations of the coating antigens, detecting antibody and the revelation process in order to improve the sensitivity of this assay. Figure **16 B** shows the results from two independent detections of aflatoxin B1 using this optimalized assay. The best sensitivity obtained with this assay was between 470 and 235 pg/ml and the inter-assay variability was below 10%.

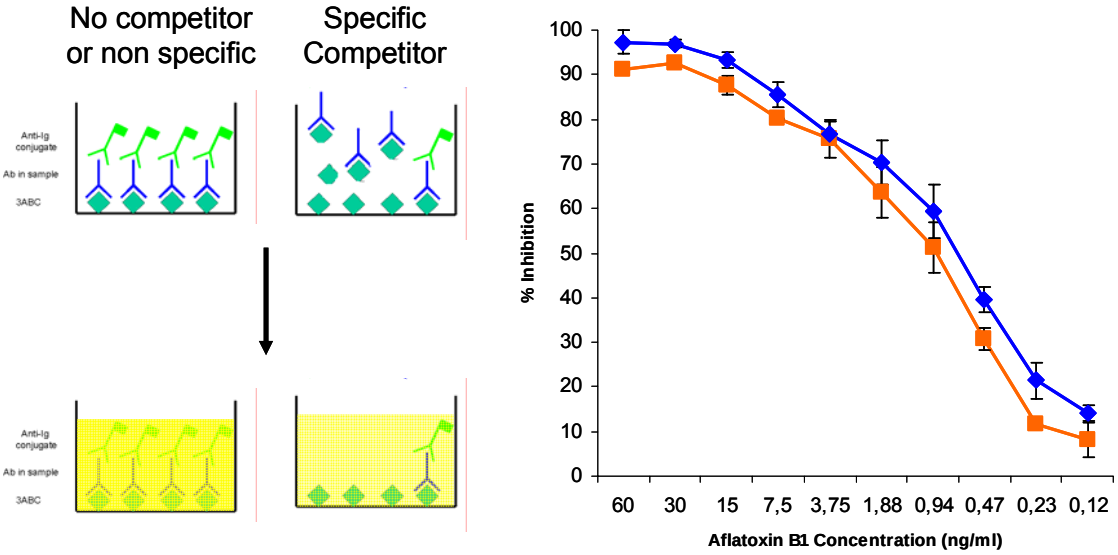


**Figure 16b**

Using this competitive ELISA we next tried to determine the concentrations of aflatoxin B1 in our environmental samples. We analysed 36 environmental samples from our collection; 15 of these were previously found to be positive in mass spectometry for the presence of aflatoxin B1. Due to the lower sensitivity of our ELISA assay as compared to the mass spectometry, we were unable to confirm the presence of the toxin in our samples. It should be noted that this lack of sensitivity of optical methods such as ELISA tests can be partially compensated by an appropriated choice of a spectral method for which a dedicated spectral range can be selected to monitor a specific binding.

## D. Production and characterisation of monoclonal antibodies against ALTERNARIA, ASPERGILLUS and STACHYBOTRYS spore fragments (Additional WP).

*This part of the report concerns new development concerning microbial compounds that were not included in the initial version of the project and that have been added at the request of BELSPO.*

Mold are very common outdoor but are also present indoor in damp places. Indeed, quantification of the mold biomass in the ambient air will be interesting in order to better appreciate the level of indoor pollution.

In order to obtain rat MoAb directed against components of the mold, LOU/c rats were immunized in the foodpats with $5.10^6$ spores of Alternaria alternata (IHEM 18586) or Aspergillus fumigatus (IHEM 6117) or Stachybotrys chartratum (IHEM 22013). At the end of the immunization, lymphocytes were obtained from the poplietal lymph nodes. Lymphocytes were fused with the IR-983F cells. Growing hybridomas were selected in HAT medium. Positive clones were selected by fluorocytometry on various mold spores.

Five MoAb were selected from the rats immunized with Alternaria alternata and their characteristics are listed on Table 3. LO-ALT-1, -3 and -5 bind alternaria spores in cytometry and also recognize alternaria mold extract using an indirect ELISA. These MoAb are all IgM. LO-ALT-2 and -5 do not recognize mold extract by ELISA and are IgG2c and IgG1 respectively.

| | Isotype | Spores cytom | Extrait Elisa |
|---|---|---|---|
| LO-ALT-1 | IgM | Y | Y |
| LO-ALT-2 | IgG2c | Y | N |
| LO-ALT-3 | IgM | Y | Y |
| LO-ALT-4 | IgG1 | Y | N |
| LO-ALT--5 | IgM | Y | Y |

**Table 3:** Characteristics of the rat MoAb obtained after an immunization with alternaria spores.

The specificities of LO-ALT-1, -3 and -5 were further analysed using fluorocytometry (Figure 17). LO-ALT-3 binds to alternaria spores IHEM 18586 but also to four other alternaria strains. However this antibody do not bind cladosporium, penicilium, aspergillus, stachybotrys nor candida and saccharomyces strains demonstrating that LO-ALT-3 is clearly species specific (while this antibody also recognize ulocladium

botrytis IHEM 328, which are phylogenically very close to alternaria ssp). The two other MoAb (LO-ALT-1 and -5) do recognize all mould strains tested until now but not yeast strains tested (Candida albicans IHEM 3731 and Saccharomyces cerevisiae IHEM 6272) indicating that this two antibodies recognize an antigenic determinant common to the moulds.

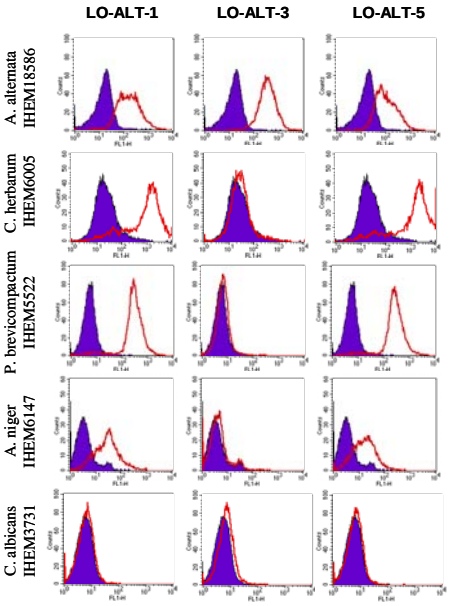


**Figure 17 :** Fluorocytometric analyse of the specificities of LO-ALT-1, -3 and -5. Mould spores were incubated with the indicated antibodies. After washing bound antibodies were detected using an FITC labelled mouse MoAb directed against the rat kappa light chains. The fluorescence was analysed on a FACscalibur cytometer.

We then analysed the ability of the LO-ALT-1 (A1) and LO-ALT-5 (F10) to detect mould componants in solution using a sandwich ELISA. Soluble extract from various mould species were prepared by overnight agitation of known numbers of mould spores in PBS. Insoluble material was removed by centrifugation. Supernatants containing the soluble antigens were tested using the various combinations of these two antibodies as capture antibody or secondary biotinylated antibody. As shown in Figure 18, the four antibody combinations tested similarly detected antigens presents in the extract of Cladosporium herbarum (IHEM 6005) but the best results were obtained with LO-ALT-5 both as a capture and as a detecting antibody.

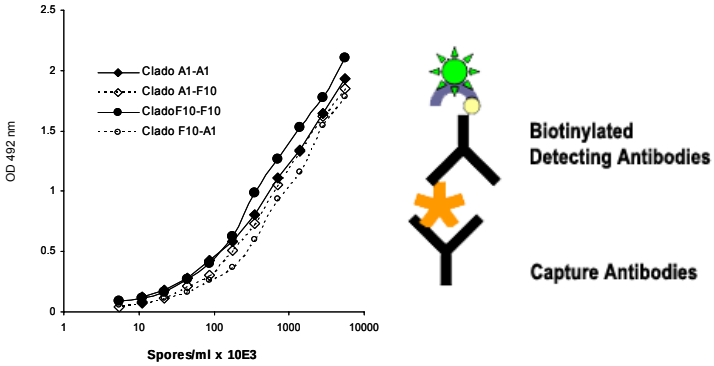


**Figure 18 :** Detection of Cladosporium herbarum extracts using a sandwich ELISA with the LO-ALT-1 (A1) and LO-ALT-5 (F10) as capture and detection antibodies. The detection antibody was labelled with biotin. Plates were revealed using peroxydase labelled avidin and OPD as substrate.

A sandwich ELISA using the LO-ALT-5 both as a capture and as a detection antibody was used to detect the presence of the recognized antigen into various mould extract preparations. As shown in Figure 19, this assay was able to efficiently detect a mould antigen in the extracts from Alternaria alternata (IHEM 21999), Cladosporium herbarum (IHEM 6005), stachybotrys chartratum (IHEM 22013), Penicillium chrysogenum (IHEM 220859). Aspergillus niger (IHEM 6147), Acremonium strictum (IHEM 19179) and Fusarium oxysporum (IHEM 3014) extracts were moderately recognized while extracts from Candida albicans (IHEM 3731) and saccharomyces cerevisiae (IHEM 6272) were not or almost not recognized.

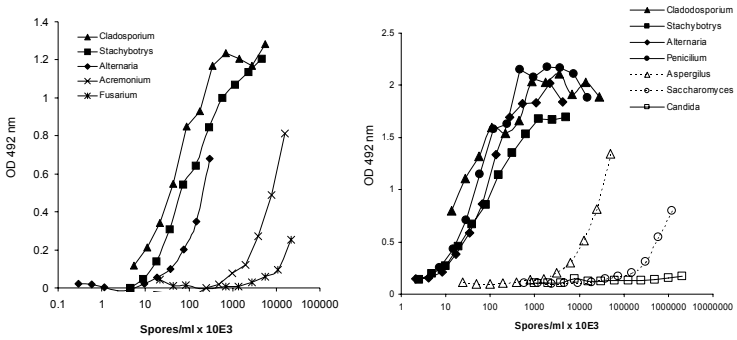


**Figure 19 :** Analysis of various mould extracts using a sandwich ELISA with the LO-ALT-5 as capture and biotin labelled LO-ALT-5 as detection antibody. Plates were revealed using Peroxydase labelled avidin and OPD as substrate.

Next we analysed the ability of this same assay to detect the antigen in environmental samples. The Figure 20 gives an example of such an experiment. One hundred centimetres square surface from ten different living rooms were vacuum cleaned and the dusts were solubilised in PBS. The quantity of LPS in these extracts was estimated by the limulus assay and the number of gram negative bacteria by standard microbiological cultures. Moreover the number of gram negative bacteria in 40 air litres of these living rooms was also estimated.

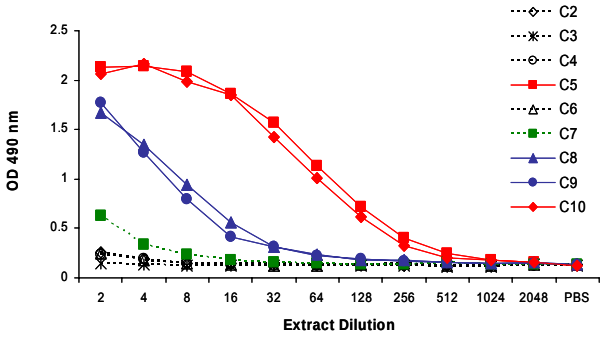


| | LPS EU /100cm 2 | BGN/ 100 cm2 | Bact/40 litres air |
|---|---|---|---|
| C5 | 105.84 | 2160 | 74 |
| C10 | 397.76 | 144 | 109 |
| C8 | 3.4 | 46080 | 17 |
| C9 | 442.56 | 1152 | 57.5 |
| C7 | 40.68 | 2240 | 187.5 |
| C2 | 13.84 | 20000 | 29 |
| C3 | 5.36 | 880 | 16 |
| C4 | 7 | 80 | 10 |
| C6 | 4.16 | 7200 | 71 |

**Figure 20 :** Analysis of various environmental samples using a sandwich ELISA with the LO-ALT-5 as capture and biotin labelled LO-ALT-5 as a detection antibody. Plates were revealed using Peroxydase labelled avidin and OPD as substrate. In the table the quantity of LPS and the number of gram negatives bacteria in the samples and the number of gram negatives bacteria in 40 litres of air.

As shown in Figure 20, the ELISA with LO-ALT-5 was able to detect the presence of an antigen in four out of the ten samples. Moreover the positives samples in ELISA were the most contaminated since they presented the highest level of LPS (samples C5, C10 and C9) or a very high number of gram negative bacteria (C8). Therefore the LO-ALT-5 antibody seems very interesting to detect a large array of mould species in environmental samples.

Six other MoAbs have been selected from rats immunized with Aspergillus. From these six antibodies LO-ASP-2 demonstrated a very good binding on Aspergillus niger (IHEM 6147) spores and a low binding to Alternaria, Cladosporium and Stachybotrys spores. Five others MoAbs have been obtained from rats immunized with Stachybotrys (Figure 21). These antibodies need to be better characterized before to be used in our biosensor.

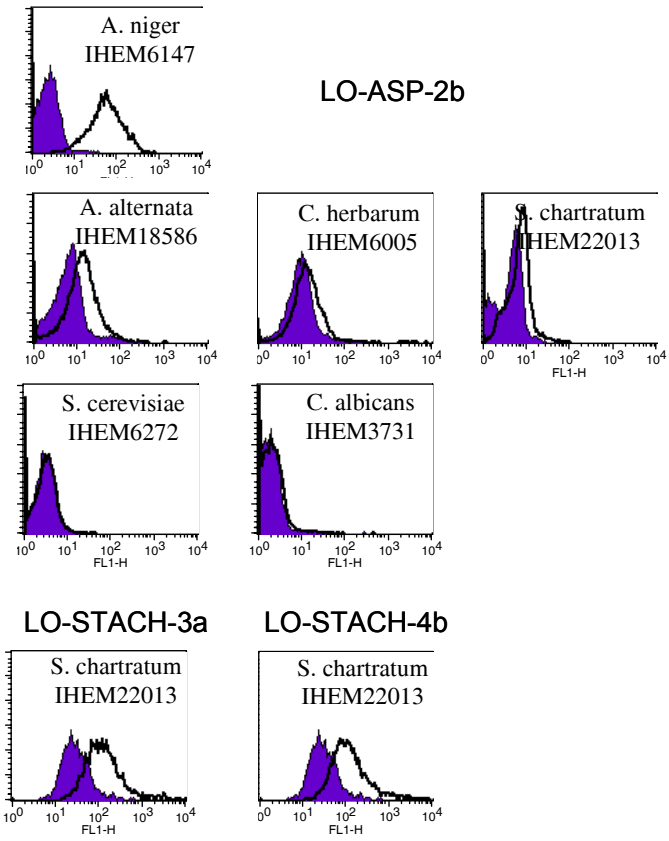


**Figure 21 :** Fluorocytometric analyse of the specificities of LO-ASP-2b on various mold species and of the binding of LO-STACH-3A and -4b on Stachybotrys spores.
Mould spores were incubated with the indicated antibodies. After washing bound antibodies were detected using an FITC labelled mouse MoAb directed against the rat kappa light chains. The fluorescence was analysed on a FACscalibur cytometer.

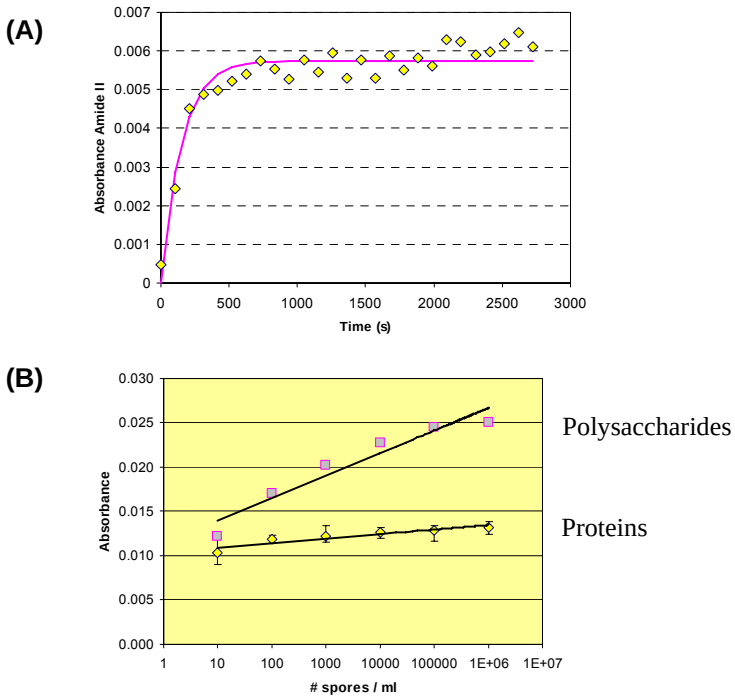


**Figure 22 : (A)** Binding of the anti-Alternaria MoAb. **(B)** Optical response of the sensor as a function of the dilution of the Alternaria extract, in the polysaccharides and in the protein spectral region.

The anti-Alternaria MoAbs were successfully immobilized at the surface of the optical sensor (Figure 22A) and their spectral response monitored, as a function of the dilution of the Alternaria extract, in the polysaccharide and in the protein spectral domains (Figure 22B). Preliminary results show that the antibodies mainly respond to the polysaccharide part of the antigen.

## E. Production of monoclonal antibodies against mycotoxins (WP3)

Mycotoxins are small non proteinic components that are not able to induce the production of antibodies when injected "as this" in animals since the production of antibodies (at least for non repetitive antigens) requires the help of T helper cells recognizing linear peptides. Indeed the activation of B cells, their production of antibodies and the generation of MoAb upon immunization requires the conjugation of the toxins to carrier proteins.

Therefore Roridin A and Verrucarin A were conjugated to the KLH and OVA. Since these toxins do not have a functionnal group to facilitate their conjugations, they were treated with succinic anyhydride to generate bis-hemisuccinate. An activated N-hydroxysuccinimide intermediate of the toxins-hemisuccinate was synthesized. Protein toxins conjugates were then prepared by coupling the activated ester reactive intermediate to the carrier's proteins using N,N′-Dicyclohexylcarbodiimide. An antiserum prepared in rabbit by the injection of satratoxin G conjugated to the BSA was prepared and was used to control the conjugation of the carrier proteins by ELISA (Figure 23). This rabbit antiserum efficiently detected OVA or KLH labelled with the roridin A toxin but not unconjugated carrier proteins indicating that our conjugation strategies were efficient. Similar results were obtained with the verrucarin A.

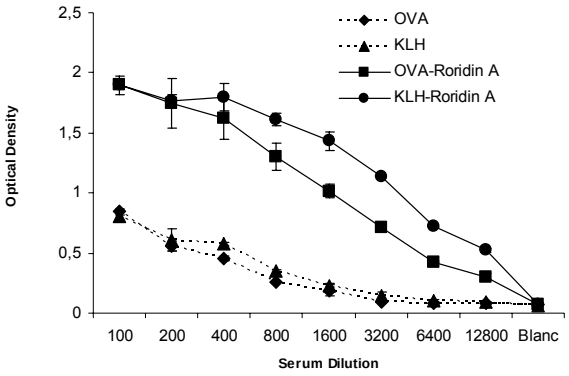


**Figure 23 :** Analysis of the toxin conjugation using an indirect ELISA with a rabbit antiserum directed against satratoxin G but crossreacting with roridin A and verrucarin A. Bound antibodies were detected using a peroxydase labelled rat MoAb directed against rabbit IgG and OPD as substrate.

LOU/c rats were immunized in the foodpats with 50 µg of roridin A or verrucarin A conjugated to the KLH. At the end of the immunizations, lymphocytes were obtained from the poplietal lymph nodes. Lymphocytes were fused with the IR-983F cells. Growing hybridomas were selected in HAT medium.

The efficiency of the immunization/fusion was confirmed by the presence of numerous clones specific for the KLH. More than 300 clones have been obtained and analysed. More than 60% of these clones were specific for the KLH but none were directed against the mycotoxins.

Therefore we decided to use another coupling reaction. We still generated a bis-hemisuccinate of the roridin A or the verrucarin A and these products were immediately coupled to the proteins (BSA, OVA or KLH) using a water soluble carbodiimide (1-ethyl-3-(3-dimethylaminopropyl)carbodiimide hydrochloride).

LOU/c rats were immunized in the foodpats with 50 µg of verrucarin A conjugated to the BSA. Poplietal lymph node cells were fused to IR-983F cells. Growing hybridomas were selected in HAT medium and their supernatants were tested by ELISA on plated coated with BSA (to monitor for the secretion of antibodies specific to the carrier) or plates coated with BSA-Verrucarin A to detect mycotoxin specific antibodies.

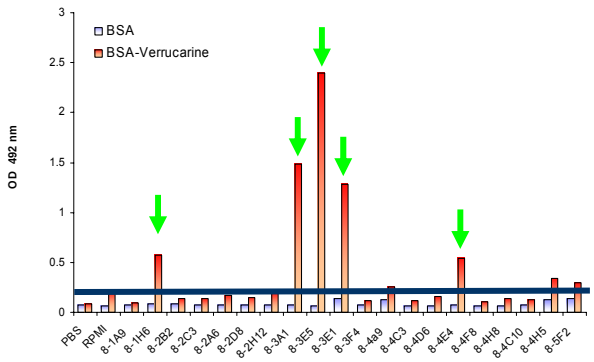


**Figure 24 :** Screening of hybridomas supernatants on ELISA plates coated with the BSA or BSA-verrucarin A.Bound antibodies were detected using a peroxydase labelled-mouse MOAb directed against rat Kappa light chains and OPD as substrate.

The Figure 24 shows the results obtained with some of these supernatants.

Astonishingly no antibody specific for the carrier was detected while antibodies specific for the mycotoxins were obtained (clones secreting antibodies in their supernatants recognizing verrucarin A modified BSA but not unmodified BSA). These results indicate that carriers were probably highly substituted and their structures very modified by the conjugation reaction. Nevertheless 8 different MoAb recognizing the mycotoxins were obtained. Supernatants from some of these clones contained antibodies recognizing verrucarin A in the context of different carriers (BSA, OVA and KLH). Some antibodies were also cross-reactive against the roridin A. An example of the results obtained with the supernatants of 3 different clones is shown on the Figure 25 and a summary of the results with the supernatants from the 8 clones is shown on the table 4.

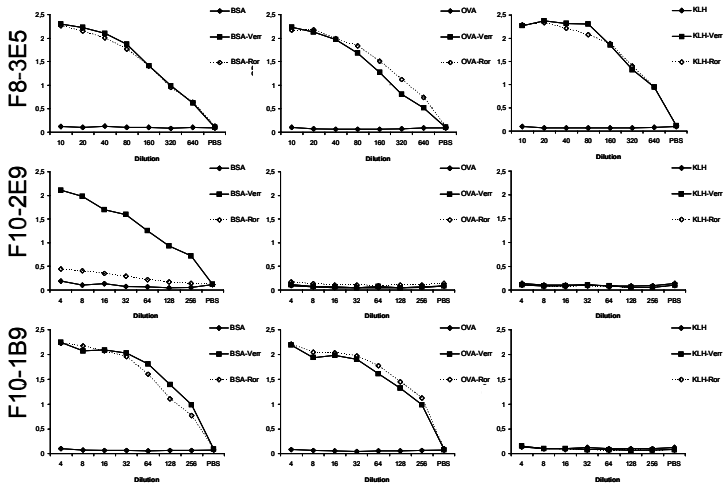


**Figure 25** : Analysis of the specificities of 3 different MoAb. Optical densities obtained from an indirect ELISA on microplates coated with the indicated proteins.After saturation, serial dilution of the indicated antibodies was applied. Bound antibodies were detected using a peroxydase labelled-mouse MOAb directed against rat Kappa light chains.

Two MoAb (F8-3E5 and F14-3G8) recognized both verrucarin A and roridin A coupled to BSA, OVA and KLH. Three MoAb recognized both mycotoxins on BSA and OVA but not on KLH. Three others were not cross-reactives and only recognized the toxin used for the immunization (verrucarin A) in the context of the carrier used (BSA). These results indicate that these three groups of antibodies could recognize three distinct epitopes on the toxins.

| Nom | Isotype | BSA | BSA-Ver | BSA-Ror | OVA | OVA-Ver | OVA-Ror | KLH | KLH-Ver | KLH-Ror |
|---|---|---|---|---|---|---|---|---|---|---|
| F8-3E5 | IgM | No | Yes | Yes | No | Yes | Yes | No | Yes | Yes |
| F14-3G8 | IgG2a | No | Yes | Yes | No | Yes | Yes | No | Yes | Yes |
| F8-1H6 | IgG2a | No | Yes | Yes | No | Yes | Yes | No | No | No |
| F8-3A1 | IgG2a | No | Yes | Yes | No | Yes | Yes | No | No | No |
| F10-1B9 | IgG2a | No | Yes | Yes | No | Yes | Yes | No | No | No |
| F8-4E4 | IgG1 | No | Yes | No | No | Yes | No | No | No | No |
| F8-3E1 | IgG2a | No | Yes | No | No | Yes | No | No | No | No |
| F10-2E9 | IgG1 | No | Yes | No | No | Yes | No | No | No | No |

**Table 4**: Summary of the isotypes and specificities of the 8 positive clones obtained.

The five clones producing antibodies recognizing both verrucarin A and roridin A in the context of at least BSA and OVA were expanded and the antibodies were immuno-purified using a mouse monoclonal antibody specific for the kappa light chains of rat immunoglobulins. The purified F8-3E5 and F8-3A1 were labelled with biotin in order to further analyse the specificities of these antibodies. As expected purified F8-3E5, F14-

3G8 and biotinylated F8-3E5 recognized both verrucarin A and roridin A on BSA, OVA and KLH while the three other purified MoAb (F8-3A1, F10-1B9 and F10-1H6) and the biotin labelled F8-3A1 recognized both mycotoxins but only when coupled to BSA or OVA but not on KLH (Figure 26, and data not shown)

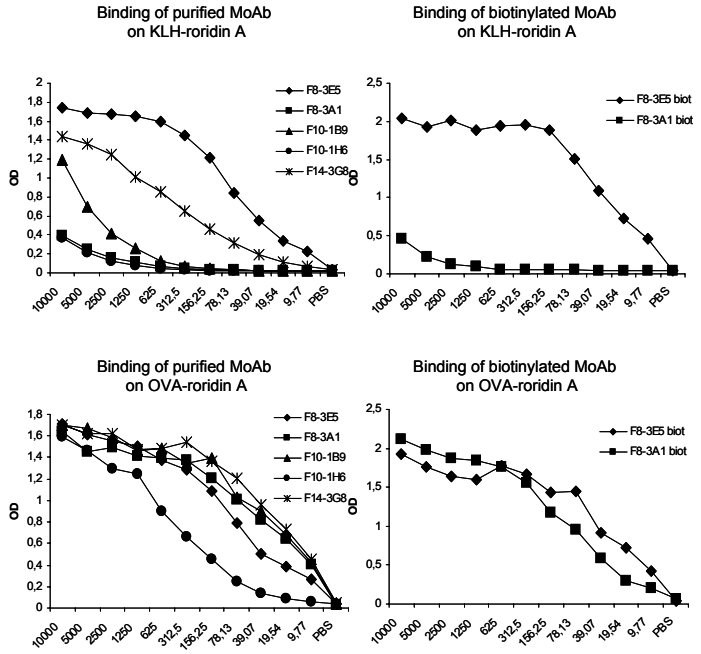


**Figure 26** : Analysis of the purified and biotinylated MoAb by an indirect ELISA. Microplates were coated with the indicated proteins. After saturation serial dilution of the indicated MoAb were applied on the plates. Bound antibodies were detected using a peroxydase labelled mouse MoAb directed against the rat kappa light chains or peroxydase labelled avidin and OPD as substrate.

We next investigated the fine specificities of these MoAb. We analysed the ability of the purified MoAb to inhibit the binding of the two biotinylated antibodies (F8-3E5 and F8-3A1) on the various toxin – carrier combinations. The Figure 27 shows an example of the results obtained.

On roridin or verrucarin coupled KLH, the binding of the biotin labelled F8-3E5 was only inhibited by this same antibody. These results demonstrate that the F8-3E5 antibody recognize a different epitope on the mycotoxins as compared to the other antibodies or that it recognize the same epitope but with a high affinity.

The biotin labelled F8-3A1 antibody as expected did not recognize the mycotoxin coupled to the KLH.

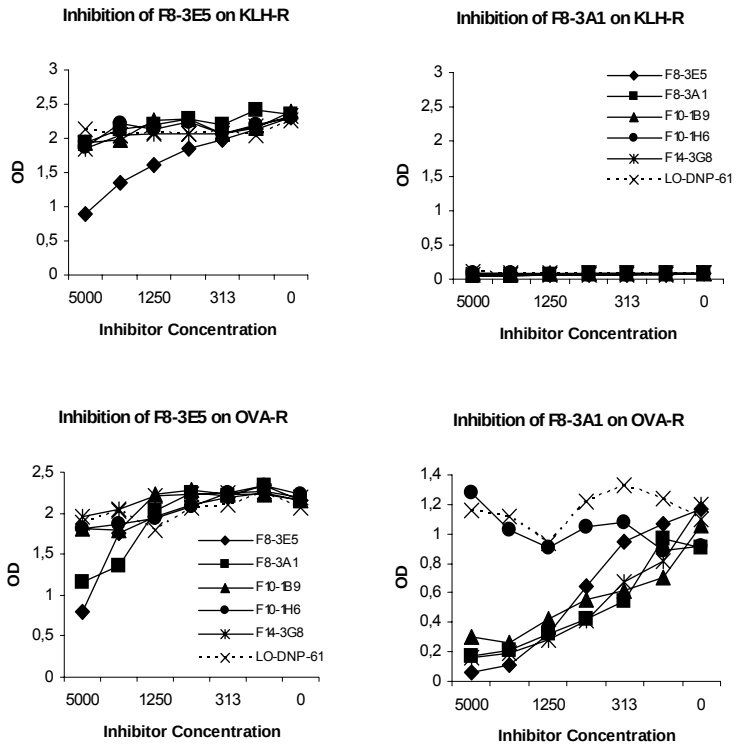


**Figure 27** : Inhibition of the binding of biotin labelled F8-3E5 and F8-3A1 by the purified rat MoAb. LO-DNP-61 was used as a negative control. Microplates were coated with the indicated proteins. After saturation serial dilution of the indicated MoAb (inhibitors) were applied on the plates together with an optimal dilution of the biotin labelled antibody (inhibited). Bound antibodies were detected using peroxydase labelled avidin and OPD as substrate.

On roridin or verrucarin coupled BSA or OVA, the binding of biotin labelled F8-3E5 was inhibited by the purified F8-3E5 and the F8-3A1. The binding of biotin labelled F8-3A1 on the same antigens was inhibited by the F8-3A1, F8-3E5, F10-1B9 and the F14-3G8. Therefore all these MoAb seem to recognize the same epitope on the mycotoxins and the lack of inhibition of F8-3E5 on roridin or verrucarin KLH is probably due to its high affinity for these antigens.

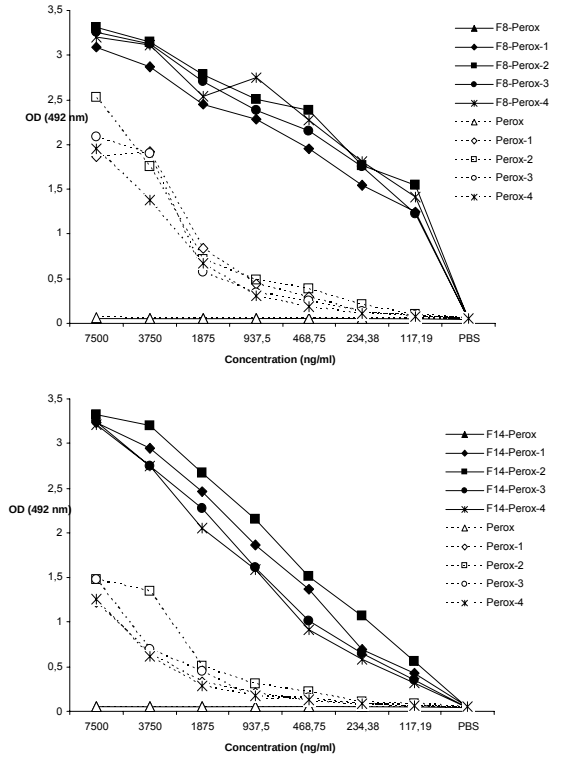


**Figure 28** : Analysis of the activity of four different conjugates of roridin A with the peroxydase. F8-3E5 and F14-3G8 antibodies were coated on microplates After saturation serial dilutions of peroxydase or mycotoxin conjugated peroxydase were applied. Bound peroxydase was detected using OPD as substrate.

Finally we started to develop a direct inhibition ELISA assay for the detection of the mycotoxins. In this kind of assay, the inhibition of the binding of an antibody to mycotoxin labelled peroxydase by free mycotoxins in the acquous phase allows the quantification of the free mycotoxins. Therefore roridin A was conjugated to the peroxydase and we realized four different conjugations with a decreasing mycotoxin / peroxydase ratio. ELISA microplates were coated with the F8-3E5 or F14-3G8 MoAb, saturated and then serial dilutions of the various conjugates were applied on the plates. As shown on the Figure 28, the four conjugates were recognized by these antibodies and the peroxydase retained its enzymatic activity after the conjugation.

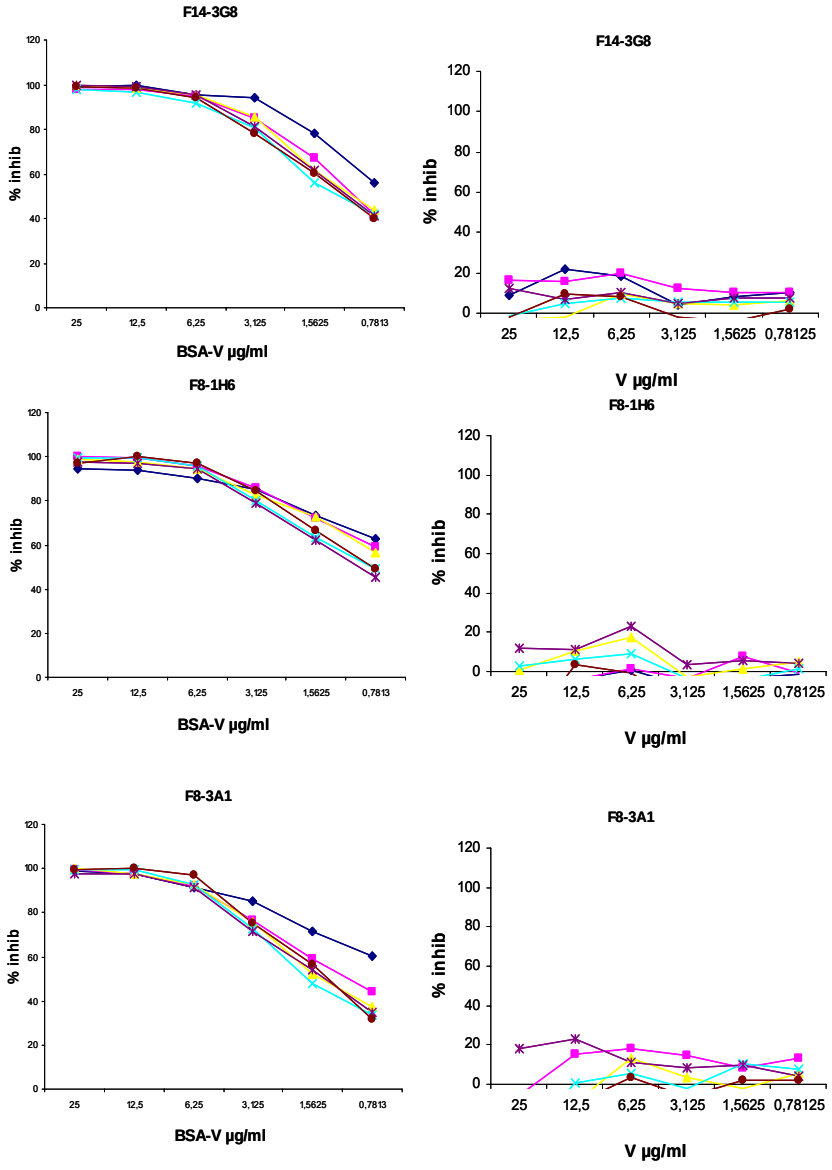


**Figure 29:** Analyse of the inhibitory activity of Verrucarin A labelled BSA and free verrucarin A in competitive ELISAs using the F14-3G8, F8-1H6 and F8-3A1 antibodies.

Using these conjugates we were able to analyse the inhibitory effect of the free and bound toxins (verrucarin A and roridin A) on the binding of toxin labelled peroxidase. As shown in figure Figure 29, BSA coupled with Verrucarin A clearly inhibited the binding of toxin labelled peroxydase to the F14-3G8, F8-1H6 and F8-3A1 (and F8-3E5 and F10-1B9 not shown) antibodies.

Unfortunately, the free verrucarin A was unable to inhibit the binding of the toxin labeleld peroxydase. Similar results were obtained using the roridin A. These results indicate that our antibodies were only detecting the coupled toxin (in a proteinic

context) but not the free toxin, therefore impeding further development of our detection assays.

Therefore we started new fusion experiments with LOU/c rats immunized in the foodpats with 50 µg of verrucarin A conjugated BSA. Poplietal lymph node cells were fused to IR-983F cells. Growing hybridomas were selected in HAT medium and their supernatants were tested by ELISA on plated coated with OVA-Verrucarin A in the absence or in the presence of 10 µg/ml of free verrucarin A (to directly monitor the binding of antibodies to the free verrucarin A). Of the 553 tested clones, 70 clones (13%) produced antibodies recognizing the verrucarin A bound to OVA. Only one of these clones produced antibodies which were inhibited by the free verrucarin A (Figure 30).

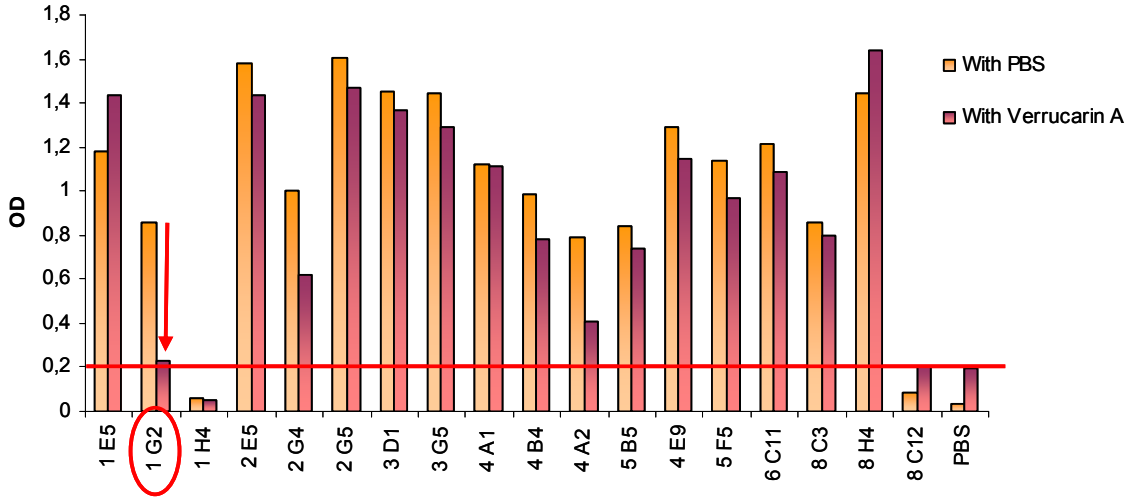


**Figure 30**: Screening of hybridomas supernatants on ELISA plates coated with OVA-verrucarin A in the presence or absence of free verrucarin A. Bound antibodies were detected using a peroxydase labelled-mouse MoAb directed against rat Kappa light chains and OPD as substrate.

The F24-1G2 antibody was then purified and its specificity was analysed in an indirect ELISA using verrucarin A or roridin A coupled BSA or OVA. This antibody was able to bind to OVA or BSA labelled verrucarin A but not to these same proteins labelled with roridin A or to the unlabelled proteins therefore demonstrating specificity towards verrucarin A only Figure 31A). In a competitive ELISA, neither free roridin A nor BSA labelled roridin A were able to inhibit the binding of the F24-1G2 antibody to BSA-verrucarin A. However this binding was efficiently inhibited by BSA labelled verrucarin A or by the free verrucarin A (Figure 31B).

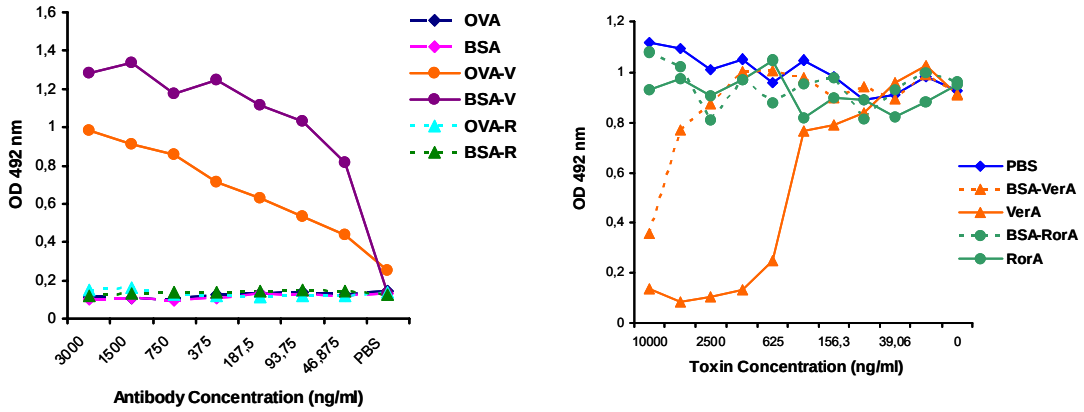


**Figure 31**: **(A)** Analyse of the specificity of the F24-1G2 antibody using an indirect ELISA. **(B)** Analyse of the inhibitory activity of the various carrier coupled toxins in a competitive ELISA using the F24-1G2 antibody.

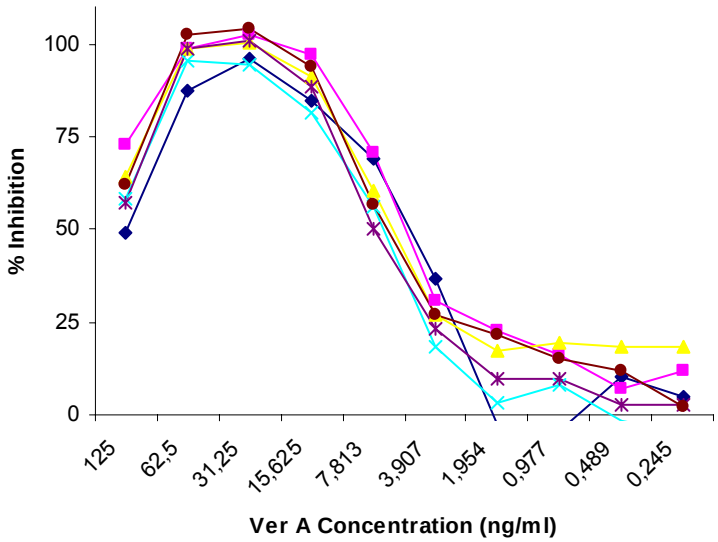


**Figure 32**: Optimalised competitive ELISA for the detection of the free verrucarin A. Six different competitions are shown.

We therefore decided to optimize this competitive ELISA in order to improve the sensitivity of this assay. We optimized the concentrations of BSA-verrucarin A for the coating, the detecting process with the F24-1G2 and the revelation process in order to improve the sensitivity of this assay. Finally we obtained sensitivity between 3.9 and 1.9 ng/ml of free verrucarin A. In the next step we will use this assay in order to detect the verrucarin A in our environmental samples.

## F. Environmental sampling (WP3)

During the first semester 2008, about 40 sampling were carried out in contaminated houses. The airborne toxins were collected on quartz filters (pore diameter: 2.2 µm) by sucking an air volume corresponding to that of ½ of the space at a flow rate of 400 L/min. In parallel to the development of our analytical tools, a cross-validation was requested at the University of Ghent (Prof. S. De Saeger) who analyzed the samples by LC-MS-MS.

In 15 of these 40 samples, mycotoxins were readily detected as concentration statistically significant. Unexpectedly, Aflatoxin B1 was also found, shedding a new light on WP2, which becomes for these reasons of great importance.
A comparison was also carried out with the commercial ELISA test Envirologix®. Discrepancies between LC-MS-MS results and ELISA results are important and the former seems to systematically under-evaluate the contamination.
Concomitantly, about 40 samples were also collected in non-contaminated houses, following the sampling procedure previously described, in order to dispose from a "blank" database.

## 4. PRELIMINARY CONCLUSIONS AND RECOMMENDATIONS

After 24 months, the **preliminary conclusions and recommendations** are the following :

- The **technology transfer** between UMons and HVS successfully occurred. Moreover, from the basics experiments related to the project scope, quality control FTIR spectrophotometers, like Nicolet 380, are shown to be adapted to BIA-ATR technology.

- On the **DNP model system**, an inhibition optimized ELISA test has been set-up, with a comparison between free DNP and DNP coupled to albumin. The level of free DNP detection was located between 4 and 8 ng/mL. In the FTIR experiments, although the binding of the MoAb was successfully monitored for all the tested MoAb, the binding of free DNP molecules was not observed in a direct testing procedure. This was explained by the relatively poor affinity of the MoAb for the free DNP molecules. According to those results, the FTIR testing methodology was changed. Immuno-assays concepts have been successfully transferred to FTIR sensors domain, yielding a new sensors category: FTIR immuno-sensors. The results relevant of these topics have been summarized in a publication: GOSSELIN E., GOREZ M., VOUE M., DENIS O., CONTI J., POPOVIC N., VAN CAUWENBERGE A., NOEL E., and DE CONINCK J. **Fourier transform infrared immunosensors for model hapten molecules**. Biosensors and Bioelectronics, 24, 2554-2558.

- As for anti-DNP MoAb, the **binding of the anti-aflatoxin antibodies** is successfully monitored in the FTIR experiments. Inhibition tests are ongoing.

- **Monoclonal antibodies against Alternaria, Aspergillus and Stachybotrys were produced and partially characterized.** In particular, we have developed and characterized two antibodies (LO-ALT-1 and LO-ALT-5) specific for an antigen present at the surface of mould spores and another antibody (LO-ALT-3) recognizing an antigen specific for Alternaria alternata and a close relative Ulocladium botrys. None of these antibodies bind to yeast spores. We have shown that LO-ALT-1 and LO-ALT-5 can be used in a sandwich ELISA to detect the presence of mould antigens in environmental samples. We have started to produce and purify these antibodies in order to use them in our biosensor device to quantify the mould biomass indoor. Use of these antibodies is ongoing using the FTIR immunosensors technology which allows an identification of the ligand.

- **The production of MoAbs against mycotoxins is ongoing.** We have also produced five cross-reactive rats MoAb recognizing both the roridin A and the verrucarin A. One antibody, the F8-3E5 seems to recognize these toxins with the highest affinity. Our inhibition assay indicates that these five antibodies recognize the same or very close epitope(s) on the mycotoxin and this result is in accordance with the relatively small size of these molecules. The F8-3E5 and the F14-3G8 antibodies are currently produced in vitro and purified to be used in our biosensor.

**Environmental sampling started Jan. 2008 and is ongoing.** Cross-validation has been carried out with LC-MS-MS technique, as well as with ELISA (Envirologix®). The latter technique seems to systematically under-evaluated the contamination level.

## 5. PROSPECTS AND PLANNING FOR PHASE 2

Until the end of Phase 2, the work plan will be the following, in agreement with the milestones and the deliverables summarized in the initial research proposal :

a) WP1 : detection of DNP - No action anymore
b) WP2 : detection of Aflatoxin B1 – set-up on the competition test for Afla B1 (determination of the sensitivity of the test, measurements on environmental samples is ongoing)
c) WP3: detection trichothecenes – Primary characterization of the binding of the antibodies on the optical platform.
d) WPx: detection of fungal spore fragments … - Analysis of the results and determination of the IR signature of the antigens.

In particular, the next step will be the characterization of the antibodies directed against stachybotrys and aspergillus already produced and their production and use in the biosensor. We will also analyse the cross-reactivities of our anti-roridin a and verrucarin A antibodies against other trichothecenes and develop a competitive ELISA assay able to detect the trichothecenes to compare the obtained results with those of the biosensor. We will also continue to produce rat MoAb against mycotoxins and immunize rats with other trichothecenes in order to generate rat MoAb with new specificities able to be used in our biosensor.

## 6. PUBLICATIONS / VALORISATION

### 6.1. Publications of the teams

#### *6.1.1. Peer review*

Fourier transform infrared immunosensors for model hapten molecules. E. Gosselin, M. Gorez, O. Denis, J. Conti, A. Van Cauwenberge, E. Noel, J. De Coninck and M. Voué, Biosensors & Bioelectronics., 24, 2554-2558 (doi:10.1016/j.bios.2009.01.001 ).

All research teams are represented.

#### *6.1.2. Others*

Detection of small molecules in competitive immunoreactions monitored by BIA-ATR sensors. E. Gosselin, M. Gorez, M. Voué, O. Denis, J. Conti, A. Van Cauwenberge, E. Noel, J. De Coninck, electronic proceedings of the EUROSENSORS 2008 Congress – Dresden – Germany (07.09-10.09.2008). (4 pages article)

All research teams are represented.

### 6.2 Other activities

Participation to the following scientific meetings :

- Rapid Methods Europe 2008 for Food and Feed Safety and Quality, January 23-28, 2008 – Noordwijk-aan-Zee – The Netherlands
- World Of Mycotoxin Forum, the Fifth Conference, Noordwijk-aan-Zee, November 17-18, 2008, The Netherlands.

Organisation of scientific meetings:

- Symposium "Indoor Air Pollution and Health Problems", Brussels, 25 May 2009, Belgium.

## 7. SUPPORT TO THE DECISION

Although quite preliminary, the results acquired during the first 24 months of the research mainly allow us to confirm the need of powerful tools such as FTIR sensors to analyze rapidly indoor pollution and to identify its chemical nature. Other commercial detection kits lack in sensitivity and in identification of the contaminants.

Nevertheless, no standardization procedure exists for evaluation of indoor pollution and the development of the technology platform by the MIC-ATR research consortium is a first step in this direction. This technological platform, on the basis of the advances done by the research group of ISP-WIV in terms of production of monoclonal antibodies and the both research groups in Mons in terms of development of FTIR-immunosensors, should be ready by the end of 2009.

The experimental platform will be extensively used during the last 12 months of the research contract to systematically evaluate the contamination level of houses in the Province of Hainaut. Comparison will be drawn with non-contaminated houses. Such a transversal study can be considered as the first step of a further epidemiologic campaign that could be carried out in a forthcoming project with the help of the Scientific Institute for Public Health.

## ANNEX 1 : FOLLOW-UP COMMITTEE

| | |
|---|---|
| Pierre Bartsch | FARES |
| Catherine Bouland | Institut Bruxellois pour la Gestion de l'Environnement |
| Joël Demarteau | Advanced Array Technology sa |
| Alexandre Legrand | Université de Mons - Hainaut |
| Sophie Lokietek | Ministère de la Communauté française |
| Bernard Monnier | Ministère de la Région Wallonne |
| Vera Nelen | Provinciaal Instituut voor Hygiëne - Antwerpen |
| Jean-Pierre Van Vooren | Hôpital Erasme - ULB |
| Yseult Navez | SPF Santé Publique, Sécurité de la Chaîne alimentaire et Environnement Cellule Santé & Environnement |
| Hervé-Marie Bazin | Immunologie – UCL |
| Alfons Callebaut | CODA/CERVA |
| Dominique Lison | Unité de toxicologie industrielle et médecine du travail – UCL |
| Sarah Desaeger | Faculteit farmaceutische Wetenschappen Universiteit Gent (UGent) |

## ANNEX 2: COPY OF THE PUBLICATIONS

A copy of the following publication is annexed to the final report phase I. The publication list is the following:

- **MIC-ATR-Annex1-1.PDF:** 1 page abstract for *"Detection of small molecules in competitive immunoreactions monitored by BIA-ATR sensors"* (E. Gosselin, M. Gorez, M. Voué, O. Denis, J. Conti, A. Van Cauwenberge, E. Noel, J. De Coninck) to be presented at the EUROSENSORS 2008 congress – Dresden – Germany (07.09-10.09.2008).

- **MIC-ATR-Annex1-2.PDF:** 4-pages article (*"Detection of small molecules in competitive immunoreactions monitored by BIA-ATR sensors"*) for the electronic proceedings of the EUROSENSORS 2008 congress.

- **BIOS-S-08-01349.PDF:** Manuscript accepted to Biosensors and Bioelectronics (Impact factor: 5.061) – *"Fourier transform infrared immunosensors"* (E. Gosselin, M. Gorez, O. Denis, J. Conti, A. Van Cauwenberge, E. Noel, J. De Coninck and M. Voué). For original publication, see the journal web site.

All these publications are made in conformity with the MIC-ATR dissemination activities plan, approved by the MIC-ATR Follow-Up Committee (Brussels, May 30, 2008).

# DETECTION OF SMALL MOLECULES IN COMPETITIVE IMMUNOREACTIONS MONITORED BY BIA-ATR SENSORS.

**E. Gosselin [(1)], M. Gorez [(1)], M. Voué [(1,*)], O. Denis [(2)], J. Conti [(1)], A. Van Cauwenberge [(3)], E. Noel [(3)], J. De Coninck [(1)]**

[1] CRMM - Université de Mons-Hainaut - Place du Parc, 20 - B-7000 Mons, Belgium
[2] Instituut Pasteur, WIV, Allergology Unit, Engelandstraat 642, B-1180 Brussels, Belgium
[3] Hainaut Vigilance Sanitaire, Boulevard Sainctelette, 55, B-7000 Mons, Belgium

*Corresponding author: M. Voué, Phone: +32 65 373885, Fax: + 32 65 373881, michel.voue@crmm.umh.ac.be

**Keywords:** label-free detection, FTIR, immunoreactions

## INTRODUCTION

Sensors based on the molecular recognition of bio-molecules have already attracted intensive interest in many different fields such as medical diagnostics and control, environmental analysis, monitoring of biotechnological processes and quality control in food industry [1]. In a recent article [2], we reviewed some specific aspects of biodetection devices and described a new type of generic biosensors suitable for the investigation of ligand-receptor interactions. These devices were based on the high sensitivity of Fourier transform infrared (FTIR) spectroscopy. This original method was based on the grafting of bifunctional spacer molecules directly at the surface of the germanium ATR element, avoiding the deposition of an intermediate metal layer or of an inorganic layer by sol-gel technique.

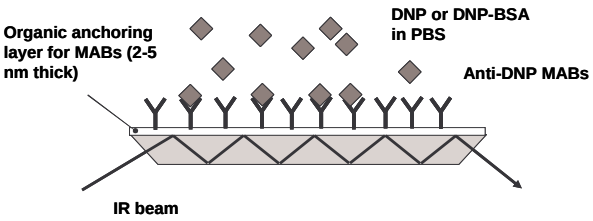


*Figure 1. BIA-ATR biosensors for immunodetection of DNP or DNP-BSA conjugates.*

2,4-dinitrophenol (DNP, Fig. 2) was considered as a model from hapten detection, but could also be used as a test molecule for explosive materials such as 2,4,6-trinitrotoluene (TNT) [3].

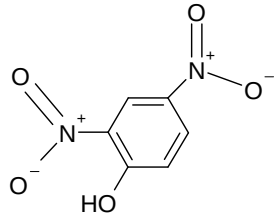


*Figure 2. 2,4-dinitrophenol (DNP)*

## RESULTS

We report experimental results concerning the detection of DNP, under its free form or coupled to bovine serum albumin (DNP-BSA), using BIA-ATR sensors. Direct as well as competitive immunoreactions were carried out using several anti-DNP monoclonal antibodies. Comparison with enzyme-linked immunosorbent assays in competition (ELISA) is given for standard operating conditions (Fig. 3).

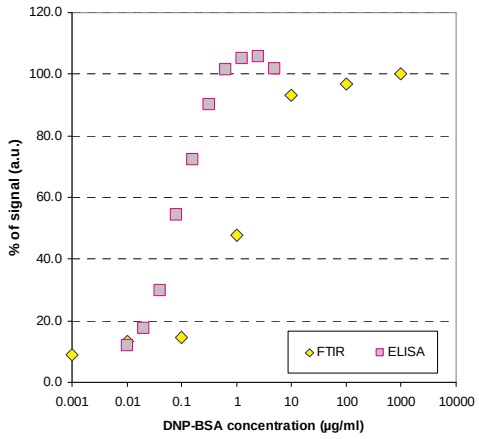


*Figure 3. Detection of DNP-BSA with LO-DNP-34 monoclonal antibodies (A: Competition ELISA test; B: direct detection with FTIR sensors)*

## REFERENCES

1. S. Andreescu, O.A. Sadik, *Pure Appl. Chem.*, 76 (2004), pp 861-878.
2. M. Voué, E. Goormaghtigh, F. Homble, J. Marchand-Brynaert, J. Conti, S. Devouge, and J. De Coninck. *Langmuir*, 23 (2007), pp 949–955.
3. H. Aizawa, M. Tozuka, S. Kurosawa, K. Kobayashi, S.M. Reddy, M. Higuchi, *Analytica Chimica Acta*, 591 (2007), pp 191-194.

(†)This work is supported by the Belgian Scientific Policy (BELSPO) in the framework of the SSD research programme (SD/HE/04A).

**Fourier transform infrared immunosensors for model hapten molecules.**

**Emmanuel Gosselin et al.**

**Corresponding author:**

**Dr. Michel Voué**

**Centre de Recherche en Modélisation Moléculaire, Université de Mons-Hainaut,**

**Place du Parc, 20, B-7000 Mons (Belgium)**

**Fax: + 32 65 373881**

**Tel: + 32 65 373885 / 83**

**Email address: michel.voue@crmm.umh.ac.be**

**Fourier transform infrared immunosensors for model hapten molecules.**

E. Gosselin [a], M. Gorez [a], M. Voué [a,*], O. Denis [b], J. Conti [a], N. Popovic [c], A. Van Cauwenberge [c], E. Noel [c], J. De Coninck [a]

(a) Centre de Recherche en Modélisation Moléculaire, Université de Mons-Hainaut, Place du Parc, 20, B-7000 Mons (Belgium)

(b) Instituut Pasteur, WIV, Allergology Unit, Engelandstraat 642, B-1180 Brussels (Belgium)

(c) Hainaut Vigilance Sanitaire, Boulevard Sainctelette, 55, B-7000 Mons (Belgium)

**Abstract**

We report experimental results concerning the detection of 2,4-dinitrophenol, under its free form or coupled to human serum albumin using Fourier Transform Infrared spectroscopy based sensors. Competitive immunoreactions were carried out using several anti-dinitrophenol monoclonal antibodies. Comparison with enzyme-linked immunosorbent assays in competition is given for standard operating conditions. FTIR detection limits are comparable to those obtained by ELISA. The limits of detection is about 5 - 15 ng/mL for the coupled DNP. Using the LO-DNP61 antibody, a detection limit of $\cong 5$ ng/mL was also estimated for the free DNP molecules but is much higher for the other antibodies.

**Key words:** biosensors, ligand-receptor interaction, FTIR, immunoreaction, monoclonal antibodies

## 1. Introduction

Sensors based on the molecular recognition of bio-molecules have already attracted intensive interest in many different fields such as medical diagnostics and control, environmental analysis, monitoring of biotechnological processes and quality control in food industry (see e.g. Andreescu and Sadik,

* Corresponding author. Fax: + 32 65 373881 - Email address: michel.voue@crmm.umh.ac.be (M. Voué).

2004, and the references therein). In a recent article (Voué et al., 2007), we reviewed some specific aspects of biosensors and presented a new type of generic device suitable for the investigation of ligand-receptor interactions. These devices were based on the high sensitivity of Fourier transform infrared (FTIR) spectroscopy. This original method was based on the grafting of bifunctional spacer molecules directly at the surface of an internal reflection element (Fig. 1), made of silicon or germanium, avoiding the deposition of an intermediate metal layer (Liley et al., 1997) or of an inorganic layer by sol-gel technique (Rigler et al., 2004; Onodera et al., 2007). Contrarily to surface plasmon resonance (SPR) or quartz crystal microbalance (QCM) sensors, FTIR sensors provide spectroscopic information concerning the chemical nature of the interacting molecules, as well as quantitative information concerning the amount of bound receptors and ligands. Furthermore, possible conformational transitions of the receptor during the interaction with its ligand can also be monitored. This information is usually not accessible using standard sensors, which only measure the mass loading of the surface. As the chemical structure of the interacting molecules is directly probed, FTIR-based sensors are *de facto* true label-free sensors.

In this article, we apply the generic FTIR sensor technology to the making of FTIR-immunosensors. The principles of theses sensors are the following: antigens coupled to proteins (typically, human or bovine serum albumin) are covalently immobilized at the sensor surface and the binding of mono- or polyclonal antibodies is monitored as a function of time, after a pre-incubation step of the antibodies with some inhibitor molecules. These sensors can readily be compared to competition enzyme-linked immuno-assays (ELISA). In particular, we have focused the research on the detection of small molecules: 2,4-dinitrophenol (DNP). Due to its low molecular weight, its chemical structure and its ability to be coupled with an immunogenic carrier, this molecule is often considered as an ideal model from hapten detection. The interest for such molecules is also due to their action as cellular metabolic poison with specific biological as well as pharmacological functions. 2,4-Dinitrophenol acts as a protein ionophore because of its ability to bind protons at one side of the plasma membrane and to release them at the other side. The consequence of this proton transfer is that, at high concentrations of DNP in the cellular environment, it becomes impossible to maintain a proton gradient with direct

influence on the oxidative phosphorylation into mitochondrial membranes (see e.g. Sibille at al., 1995 and the references therein). For these reasons and its action on fatty acid synthesis (Rossmeisl et al., 2000), DNP has been used in the early 30s as a pharmacological treatment of overweight patients (Bray and Greenway, 2007; Adan et al., 2008) but induced unattended consequences such as cataracts, neuropathy or cardiac failure. An interesting application of this chemical compound was recently reported by De Felice and coworkers: its anti-amyloidogenic effect (De Felice et al., 2001 and 2004; Wasilewska-Sampaio et al., 2005). These authors have shown that DNP acts as a blocking agent in the formation of both soluble oligomers and insoluble amyloid fibrils from the β-amyloid peptide, the main neurotoxin involved in the pathogenesis of Alzheimer's disease. They summarize this effect as 'the gentle face of Janus', a reference to Roman mythology because this neuroprotective properties are opposite to the toxicity at high concentrations of 2,4-dinitrophenol and other nitrophenols (De Felice et al., 2006).

Some attempts have been carried out to functionalize porous silicon for immunosensor application but the binding of the antigens was monitored by measuring the capacitance–voltage curve in cyclic voltametry (Meskini et al., 2006), by SPR (Aizawa et al., 2007) or by QCM (Park et al., 2001; Park et al., 2003; Kurosawa et al., 2003). Recently, Salmain and coworkers (2008) presented results concerning the detection of herbicide atrazine using a sensor based on reflection–absorption infrared spectroscopy (RAIRS) coupled to polarization modulation (PM). This technique is similar to infrared Fourier transform ellipsometry (FTIR-SE) (Tompkins and Irene, 2005; Dahmouchene et al., 2008), although neglecting the phase change occurring during the reflection of the infrared beam at the sensor surface but our study is the first one considering the covalent binding of antigen/carrier couples on semi-conductor elements in conjunction with the detection of the antigen/antibody interactions using FTIR in total attenuated reflection (ATR) mode.

## 2. Experimental techniques

Unless otherwise stated, the purchased chemicals are of analytical grade and were used as received, without further purification. Anti-DNP monoclonal antibodies were purchased from IMEX (Belgium).

The isotypes of the LO-DNP01, LO-DNP34 and LO-DNP61 anti-DNP monoclonal antibodies are respectively: IgG1 kappa, IgM kappa and IgG2a kappa. DNP and its complexed form with a carrier protein (DNP-HSA) were purchased from Sigma-Aldrich. For the latter molecule, the coupling ratio was 30-40/1, according the manufacturer's information. Phosphate buffered saline (PBS, 0.010 M pH 7.4) solution was prepared from Sigma Aldrich dry powder.

*2.1. FTIR biosensors.*

The FTIR biosensors were prepared according to the procedure described by Voué et al. (2007). The main steps of the infrared element cleaning and functionalization are summarized hereafter.

*a) Cleaning and activation:* The internal reflection elements were silicon ATR prisms (ACM, Villiers St Frédéric, France) with an aperture angle of 45°. They were degreased in chloroform (2 x 5 min) under sonication. Each face of the crystal was exposed to UV radiation in a UV-ozone cleaner (PR100, UVP, England) during 10 min to remove the surface organic contaminants. The crystals were activated in a mixture of $H_2O_2 – H_2SO_4$ (7:3 v:v) during 8 min at 150°C before being abundantly rinsed in MilliQ water and dried under a $N_2$ flux. Final activation was carried out in a UV-Ozone cleaner during 30 min.

*b) Grafting of OTS molecules.* The activated ATR elements were hydrophobized by grafting an octadecyltrichlorosilane (OTS, Sigma-Aldrich) self-assembled monolayer (SAM): the activated ATR elements were immersed in a solution of OTS (0.08% v:v) in a mixture of hexadecane and $CCl_4$ (ratio 7:3 v:v) for 16 h at 12 °C (Voué et al., 1999, Semal et al., 1999). The grafted elements were rinsed in chloroform (2 x 5min) under sonication. To avoid dewetting of the spacer molecules solution, the OTS-grafted surfaces were placed 2 min in a UV-ozone oven (PR100, UVP, UK) at a distance of 7 cm from the UV source. This results in a partial burning of the SAM and of an increase of ATR element critical surface tension.

*c) Grafting of the spacer molecules.* Contrarily to our previous article (Voué et al, 2007), commercial spacer molecules were used. N-Succinimidyl (4-azidophenyl) 1,3´-dithiopropionate molecules (SADP, Pierce, USA) were dissolved in acetonitrile (1.8 mg/mL). The SADP solution is sprayed on the partial-OTS surfaces. The solvent was evaporated in the dark before irradiation during 2 hrs at 7 cm of a UV

lamp ($\lambda_{max}$ = 254 nm). Photo-grafted surfaces were rinsed in acetonitrile (2 x 5 min) under sonication. The so-obtained surfaces were stable when kept in closed vials at normal storage conditions.

*2.2. FTIR experiments*

ATR-FTIR spectra were recorded on a Nicolet 6700 FTIR spectrophotometer (Thermo Electron Corporation, USA) equipped with a liquid $N_2$ cooled MCT detector at a resolution of 2 $cm^{-1}$ with a mirror speed of 0.6329 cm/s. The spectrometer was continuously purged with dry air (Parker-Zander, Germany) at a flow of 30 SCFH. The processing of the spectra was done using the OMNIC 7.3 software (Thermo Electron Corporation, USA). The SADP-functionalized surfaces were placed in an ATR flow cell (Specac, UK) connected to a Watson-Marlow 403U/VM2 peristaltic pump (Farmount, UK). Typical flow speed was 20 µL/min.

*2.3 Inhibition tests with FTIR immunosensors*

In a first step, a DNP-HSA solution (1 mg/mL in PBS) was injected in the flow cell at a flow rate of 5 to 10 µL/min (discontinuous). After 2 h, buffer solution was injected in the cell to remove the unreacted excess of protein. After the binding of the protein to the sensor surface, monoclonal antibodies (Mabs) (5 µg/mL in PBS) were incubated at room temperature in the presence of either free or coupled DNP. After 20 min of incubation, an aliquot of the Mabs/inhibitor solution was injected in the flow cell and the binding of the antibody to the immobilized protein was monitored as a function of time by recording FTIR spectra.

*2.4. Antibody detection with ELISA technique*

EIA microtitration plates (Flow laboratories) were coated overnight at 4°C (100µL/well) with a solution of albumin labelled with 2,4-DNP (DNP-HSA, Sigma) diluted (5µg/mL) in borate buffer pH 9. Plates were washed in PBS and saturated with proteins from skimmed milk for 2h at 37°C. After washing with PBS, serial twofold dilutions of free 2,4-DNP (Sigma) or albumin labelled DNP in PBS were applied on the plates (100 µL/well) together with a constant concentration (0.5 µg/mL, 100 µL/well) of various rat monoclonal antibody directed against the DNP (IMEX, UCL, Brussels, Belgium). Plates were incubated for 2h at 37°C. Then plates were washed in PBS 0.1% Tween 20 and a peroxydase labelled mouse monoclonal antibody directed against rat kappa light chains was added to the wells (MARK-1 PO, IMEX, 1 µg/mL in PBS 0.1 % Tween 20, 100 µL/well) for 2h at 37°C.

Finally plates were washed with PBS 0.1% Tween 20 and developed by the addition of 100 µL of OPD (SigmaFast OPD, Sigma). The reaction was stopped with 50 µL of 2N $H_2SO_4$ and optical densities were read at 492 nm with a model 680 microplate reader from Biorad. Percent inhibition was calculated for each inhibitor concentration according to

$$I_{ELISA} = 100\left[1 - \frac{A_i}{A_{control}}\right] \quad (1)$$

with $A_i$ and $A_{control}$ are the optical densities (OD) obtained in the presence and in the absence of the inhibitor, respectively.

**3. Results and discussion.**

*3.1. Molecular architecture of the sensor*

The organic functional layer at the surface of the silicon ATR element is build according a two-steps procedure and its thickness is about 2-5 nm. The sensor is schematically represented in Fig. 1. TFTIR spectra of the organic layer are given as supporting information in Fig. A1. The spectrum recorded on the activated (but non-functionalized) crystal is recorded and used as baseline (Fig. A1, trace **a**). Trace **b** is the FTIR spectrum relevant of the grafting of the OTS molecules. The main absorption bands are found in the C-H stretching region (3000 – 2800 $cm^{-1}$) and are characteristics of the aliphatic hydrocarbons. Theses bands, found around 2958, 2917 and 2850 $cm^{-1}$ (Fig. A1, inset), correspond to the asymmetric $CH_3$ (2980-2950 $cm^{-1}$), asymmetric $CH_2$ (2950-2873 $cm^{-1}$), and symmetric $CH_2$ (2872-2812 $cm^{-1}$) stretching bands. Taking this trace as the new baseline and photografting the SADP molecules after partial degradation of the OTS layer under UV exposure gives trace **c**. The bands characteristics of the OTS molecules appear in negative mode, as a result of the photo-degradation of the aliphatic chains, but positive peaks relevant of SADP are found around 1736, 1490, 1205 and 1150 $cm^{-1}$. The presence of these very sharp peaks, which mainly correspond to the C=O and C-O stretching absorption bands, confirms the appropriate functionalization of the surface.

*3.2. Binding of the receptors*

The functionality of the sensor is probed by binding the hapten-carrier molecular complex to the surface. Practically, the binding of DNP-HSA to the sensor surface can be quantified and monitored on-line from the FTIR intensity of some specific absorption bands (Fig. 2). Spectra were recorded every 70 s but only one spectrum over 5 is represented for clarity of the figure. As the coupling between the protein and the surface requires the hydrolysis of the activated ester of the N-succinimidyl group of the SADP molecule, 4 bands are characteristics of the appropriate anchoring of the protein at the sensor surface: the amide I and amide II absorption bands of the protein at 1644 and 1548 $cm^{-1}$ and the stretching bands ν(C=O) (1736 and 1710 $cm^{-1}$) and ν(C-O) (1209 $cm^{-1}$). Taking a baseline the spectrum recorded on the SADP-functionalized crystal surface, the amide bands appear in positive mode as they correspond to the binding of the protein, while the three latter appear in negative mode as they monitor the hydrolysis of the reactive function of SADP molecules. It should also pointed out that the shape of the absorption bands in the 1160-1040 $cm^{-1}$ region considerably evolves with time: peaks at 1098 and 1059 $cm^{-1}$ strongly increase while peaks at 1156 and 1131 $cm^{-1}$ progressively decreases. The stability of the anchored protein layer is shown in Fig. A2 (Supporting information section): the absorbance of the amide II band remains constant during rinsing of the flow cell with PBS solution. The coupling of DNP to HSA molecules occurs at the level of their peripherical $NH_2$ groups (i.e. mainly on the lysine amino-acids). They are therefore less numerous than in native albumin molecules and the amount of DNP-HSA bound to the sensor surface is less than the one of BSA (Fig. A2, open diamonds).

Besides their sensitivity and their ability to monitor the binding in real-time, FTIR sensors have another advantage: they allow differentiating bound molecules. Figure 3 represents the spectra of DNP-HSA (plain line), of bovine serum albumin (BSA, dashed line) and of anti-DNP monoclonal antibodies (LO-DNP61, dotted line). The shape of the amide bands is characteristics of the secondary structure of the protein. These three spectra stress the advantage of the FTIR-ATR approach which allows the identification of a protein among several others present in a mixture through the FTIR spectrum. Other studies reporting the spectra of more than 50 proteins have stressed the uniqueness of the IR spectrum, related to a large extent to their α-helix and β-sheet contents (Goormaghtigh et al., 2006). Goormaghtigh and coworkers (2006) proposed to determine these contents using absorbance

values measured at a restricted number of wavenumbers and (multi-)linear models, after baseline subtraction (linear baseline between 1700 and 1500 $cm^{-1}$) and either area- or point-normalization of the spectra. In that study, thin protein films were obtained by slowly evaporating a sample solution containing 100 µg of protein on one side of a cleaned ATR germanium crystal under a stream of nitrogen. In our case, the experimental protocol is different: the spectra were recorded on protein films covalently bound to the ATR element. They therefore contain, as shown in Fig. 2, the contributions of the bound protein and of the hydrolyzed spacer arms. Due to the presence of the strong (negative) bands above 1700 $cm^{-1}$, the linear model proposed by Goormaghtigh et al. can not be directly applied, although the underlying concept remains valid. Significant peaks of DNP-HSA are reported in Fig. 3. They correspond to the peaks identified for BSA but some peak displacements are observed in the spectrum of the DNP-LO61 antibody in the amide I-II region: the peak of DNP-HSA at 1643 $cm^{-1}$ and 1549 $cm^{-1}$ are shifted to 1637 $cm^{-1}$ and 1546 $cm^{-1}$, respectively. A simple déconvolution of the peaks shape in the 1700-1600 $cm^{-1}$ region (data not shown) shows that the shape of the amide I band of DNP-HSA can be adequately fitted by two components at 1657 and 1636 $cm^{-1}$ while the shape of the amide I band of DNP-LO61 is described by only one peak et 1637 $cm^{-1}$. In the DNP-HSA spectrum, the area of the peak at 1657$cm^{-1}$ approximately corresponds to 35% of the area of the amide I band. This result has to be compared with the content in α-helix of ovalbumin (≅30%) (Goormaghtigh et al., 2006). The absence of the peak at 1657 $cm^{-1}$ in the DNP-LO61 spectrum shows that the α-helix content is much less than in the previous case, as expected for a monoclonal antibody. Moreover, the negative peak of DNP-LO61 at 1708 $cm^{-1}$ is less intense than in the albumin spectra and only contributes to 24% to the band area, whereas in the case of DNP-HSA, it corresponds to 59% of the band area.

*3.3. Control experiments*

Up to now, we have shown the molecular construction of the sensor and its ability to covalently bind molecular receptors: the DNP-HSA molecules. Two types of complementary experiments were carried out to check the saturation of the unreacted sites and the specificity of the molecular recognition of the DNP-HSA molecules by the anti-DNP monoclonal antibodies. Their results are presented in the Supporting information section (Fig. A3) and are only briefly summarized hereafter. On one hand, the

absence of covalent binding of concentrated glycine at the level of a DNP-HSA sensor surface allows us to conclude that the sensor surface is covered at more than 95% by the initially bound protein layer (Fig. A3a). On the other, the specificity of the molecular recognition of the anti-DNP Mabs was shown by their lack of binding to an avidin-covered sensor surface (Fig. A3b).

*3.4. Competition assays*

A series of inhibition tests was carried out to probe the sensitivity of the detection method with respect to the coupled or to the free DNP. After binding the coupled protein to the sensor surface, solutions containing Mabs and inhibitors were injected in the flow cell after 20 min of incubation at room temperature. The absorbance of the sample is easily converted in percentage of inhibition by

$$I = 100\left(1 - \frac{A_i - A_0}{A_{\max} - A_0}\right) \quad (2)$$

where $A_i$ is the absorbance of the sample, $A_0$ is the absorbance measured after the binding of the protein and the subsequent rinsing with PBS and $A_{max}$ the absorbance measured in the absence of inhibitor. In each case, the absorbance refers to the amide II band.

We considered two types of inhibitors: free DNP and DNP-HSA molecules. Using this experimental scheme, three monoclonal antibodies against DNP were tested: LO-DNP61, LO-DNP34 and LO-DNP01. The results presented in Figure 4 clearly show that these antibodies respond in a different manner to the free or to the coupled molecule. The sensitivity is about 10 to 100 times higher for the coupled molecule than for the free antigen (Fig. 4a). More interesting is the fact that the response of the test also depends on the antibody for the free antigen, although the responses are equivalent for coupled DNP. In the case of free DNP, the LO-DNP34 has sensitivity about 100 times less than the other types of antibodies. It should also be pointed out that the LO-DNP61 antibodies interact with the free DNP molecules (Fig. 4a, filled circles) in a way similar to the one they interact with the hapten-carrier complexes, at least at low concentration of inhibitors.

Similar experiments were carried out using ELISA technique. Their results are presented in Fig. 4b. The curves are steeper than for the FTIR sensors. All the tested antibodies respond in a similar manner to the coupled DNP molecules (open symbols) but significant differences are observed for the

recognition of free DNP molecules (filled symbols). Sensitivity is about 100 times higher for LO-DNP61 but LO-DNP34 does not recognize the free DNP molecules.

All the inhibition data sets represented in Fig. 4a and b can be modelled by a sigmoid equation whose parameters are log $EC_{50}$, the logarithm of the concentration (in μg/mL) at which a level of 50% of inhibition is observed, and the slope of the curve at its inflexion point, usually refereed to as the Hill slope. Non-linear least-squares regression was carried out for each data set (Fig. 4a and b, plain and dashed lines) and the best-fit parameters are summarized in Table 1. These figures confirm that significant differences exist not only between the molecular recognition mechanisms of free or coupled DNP molecules by monoclonal antibodies, but also between the detection techniques (FTIR or ELISA). It should not be forgotten that, although the principles of the assays are equivalent, the experimental conditions under which they are carried out are relatively different.

Finally, starting from the values of log $EC_{50}$ and of the Hill slope, two additional parameters can be calculated: $EC_{10}$ and $EC_{90}$. They respectively correspond to the concentration at which a level of 10% and 90% of inhibition are observed. $EC_{10}$ can be considered as the limit of detection and the difference $EC_{90}$-$EC_{10}$ as the operational concentration range for the immuno-assays. For the DNP-HSA inhibitors, the limits of detection are equivalent between both techniques: in the range 5 – 15 ng/mL (FTIR assays) and about 40 ng/mL (ELISA). For the free DNP molecules, the limits of detection are different: higher than 1 μg/mL (ELISA for all the antibodies and FTIR for LO-DNP34) but detection limit of 4 ng/mL was estimated using FTIR assays and LO-DNP61 antibody, which is a level comparable to those estimated for the coupled molecules.

**4. Conclusions.**

Competitive immunoreactions were carried out using several anti-DNP monoclonal antibodies and FTIR-ATR based sensors. Two types of inhibitors (free and coupled DNP) were tested. Comparison with enzyme-linked immunosorbent assays in competition is given for standard operating conditions. FTIR detection limits are comparable to those obtained by ELISA and the limits of detection is about

5 - 15 ng/mL for the coupled DNP. Using the LO-DNP61 antibody, a detection limit of $\cong 5$ ng/mL was also estimated for the free DNP molecules.

**Acknowledgements**

This research has been supported by the Belgian Federal Science Policy Office (Science for a Sustainable Development Program – MIC-ATR project) and by the Ministère de la Région Wallonne. Thanks are due to E. Goormaghtigh, F. Homblé and J. Marchand-Brynaert for helpful discussions.

**References**

Adan, R. A. H., Vanderschuren, L. J. M. J., la Fleur, S. E., 2008. Trends Pharmacol. Sci. 29, 208-217.

Aizawa, H., Tozuka, M., Kurosawa, S., Kobayashi, K., Reddy, S.M., Higuchi, M., 2007. Analytica Chimica Acta, 591, 191-194.

Andreescu, S., Sadik, O.A., 2004. Pure Appl. Chem. 76, 861-878.

Bray, G.A., Greenway, F.L., 2007. Pharmacol. Rev. 59, 151–184.

Dahmouchène, N., Coppée, S., Voué, M., De Coninck, J., 2008. phys. stat. sol (c) 5, 1210-1214.

De Felice, F. G., Houzel, J. C., Garcia-Abreu, J., Louzada, P. R., Afonso, R. C., Meirelles, M. N., Lent, R., Neto, V. M., Ferreira, S. T., 2001. FASEB J. 15, 1297–1299.

De Felice, F. G., Vieira, M. N., Saraiva, L. M., Figueroa-Villar, J. D., Garcia-Abreu, J., Liu, R., Chang, L., Klein, W. L., Ferreira, S. T., 2004. FASEB J. 18, 1366–1372.

De Felice F. G., Ferreira, S. T., 2006. IUBMB life 58, 185-191.

Goormaghtigh, E., Ruysschaert, J.M., Raussens, V., 2006. Biophys. J. 90, 2946-2957.

Kurosawa, S., Aizawa, H., Tozuka, M., Nakamura, M., Park, J.W., 2003. Meas. Sci. Technol. 14, 1882-1887.

Liley, M., Keller, T.A., Duschl, C., Vogel, H., 1997. Langmuir 13, 4190–4192.

Meskini, O., Abdelghani, A., Tlili, A., Mgaieth, R., Jaffrezic-Renault, N., Martelet, C., 2007. Talanta 71, 1430-1433.

Onodera, K., Hirano-Iwata, A., Miyamoto, K., Kimura, Y., Kataoka, M., Shinohara, S., Niwano, M., 2007. Langmuir 23, 12287-12292.

Park, J.W., Kurosawa, S.; Han, D.S., Aizawa, H., Yoshimoto, M., Nakamura, C., Miyake, J., Chang, S.M., 2001 Proceedings of the 2001 IEEE International Frequency Control Symposium & PDA Exhibition, 489-491.

Park, J.W., Kurosawa, S., Aizawa, H., Han, D.S., Yoshimoto, M., Nakamura, C., Miyake, J., Chang, S.M., 2003. IEEE Trans. Ultrason. Ferroelectr. Freq. Control 50, 193-195.

Rigler, P., Ulrich, W.P., Hoffmann, P., Mayer, M., Vogel, H., 2003. ChemPhysChem 4, 268–275.

Rossmeisl, M., Syrovy, I., Baumruk, F., Flachs, P., Janovska, P., Kopecky, J., 2000. FASEB J. 14, 1793-1800.

Salmain, M., Fischer-Durand N., Pradier, M.-C., 2008. Anal. Biochem. 373, 61–70.

Semal, S., Voué, M., Dehuit, J., de Ruijter, M., De Coninck, J., 1999. J. Phys. Chem. B 103, 4854–4861.

Sibille, B., Keriel, C., Fontaine, E., Catelloni, F., Rigoulet, M., Leverve, X. M., 1995. Eur. J. Biochem. 231, 498–502.

Tompkins, H. G., Irene, E. A., Handbook of Ellipsometry (Springer, Heidelberg, 2005).

Voué, M., Goormaghtigh, E., Homblé, F., Marchand-Brynaert, J., Conti, J., Devouge, S., De Coninck, J., 2007. Langmuir 23, 949–955.

Voué, M., Semal, S., De Coninck, J., 1999. Langmuir 15, 7855–7862.

Wasilewska-Sampaio, A. P., Silveira, M. S., Holub, O., Goecking, R., Gomes, F. C. A., Neto, V. M., Linden, R., Ferreira, S. T., De Felice, F. G., 2005. FASEB J. 19, 1627-1636.

**Figure captions**

**Figure 1.** Schematic representation of the sensor.

**Figure 2.** Time evolution of the FTIR-ATR spectra recorded during the binding of the DNP-HSA molecules on a SADP functionalized silicon crystal. The spectra were recorded every 70 s.

**Figure 3.** Comparison of the FTIR spectra of linked proteins (plain line: DNP-HSA, dashed line: BSA, dotted line: anti-DNP Mab LO-DNP61).

**Figure 4.** Inhibition curves for DNP-HSA (open symbols) and free DNP (filled symbols) using (a) FTIR immuno-sensors and (b) ELISA – Influence of the antibody (circles: LO-DNP61, triangles: LO-DNP34, diamonds: LO-DNP01). Plain and dashed lines: best-fit results of the sigmoid equation for the coupled and free DNP, respectively. Best-fit parameters are given in Table 1.

**Tables**

**Table 1.** log $EC_{50}$ and Hill slope: best-fit parameters of the sigmoid curves for the inhibition tests.

$EC_{10}$ and $EC_{90}$: concentrations (in µg/mL) giving 10 and 90 % of inhibition.

| Testing method | Inhibitor | Monoclonal antibodies | Best-fit parameters | | Inhibitor conc. (µg/mL) | |
|---|---|---|---|---|---|---|
| | | | log $EC_{50}$ (*) | Hill slope | $EC_{10}$ | $EC_{90}$ |
| FTIR | DNP | LO-DNP61 | -0.188 ± 0.098 | 0.424 ± 0.043 | 0.004 | 115.497 |
| | | LO-DNP34 | 1.582 ± 0.128 | 0.661 ± 0.157 | 1.375 | 1060.803 |
| | | LO-DNP01 | 0.410 ± 0.113 | 0.606 ± 0.112 | 0.068 | 96.529 |
| | DNP-HSA | LO-DNP61 | -0.925 ± 0.063 | 0.724 ± 0.070 | 0.006 | 2.472 |
| | | LO-DNP34 | -0.400 ± 0.068 | 0.673 ± 0.069 | 0.015 | 10.421 |
| | | LO-DNP01 | -0.774 ± 0.094 | 0.705 ± 0.099 | 0.007 | 3.798 |
| ELISA | DNP | LO-DNP61 | 0.985 ± 0.032 | 1.017 ± 0.078 | 1.114 | 83.809 |
| | | LO-DNP34 | N.A. | N.A. | N.A. | N.A. |
| | | LO-DNP01 | 2.273 ± 0.139 | 0.452 ± 0.068 | 1.452 | $> 20\ 10^3$ |
| | DNP-HSA | LO-DNP61 | -0.555 ± 0.052 | 1.108 ± 0.131 | 0.038 | 2.024 |
| | | LO-DNP34 | -0.428 ± 0.037 | 0.986 ± 0.075 | 0.040 | 3.466 |
| | | LO-DNP01 | -0.533 ± 0.046 | 1.079 ± 0.110 | 0.038 | 2.246 |

(*) Concentrations are given in µg/mL.

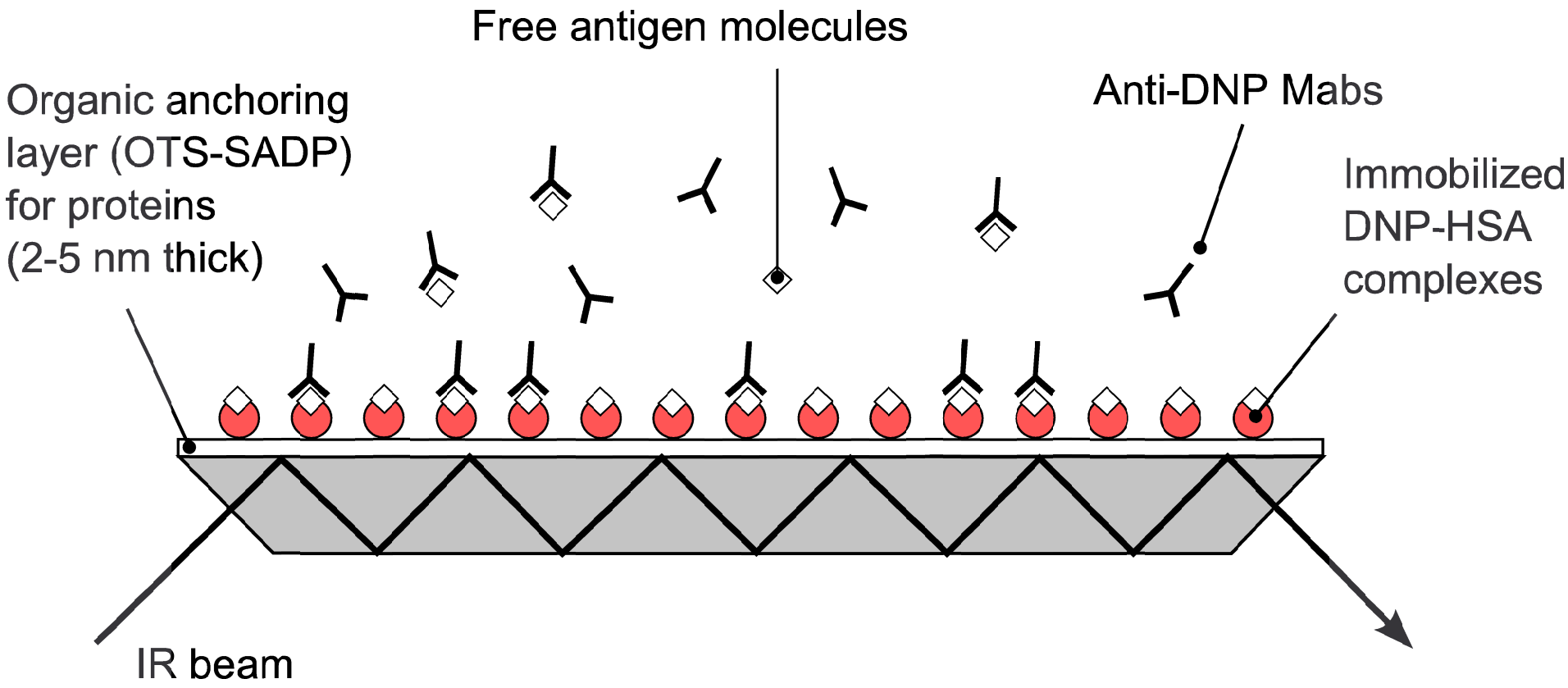
Free antigen molecules
Organic anchoring layer (OTS-SADP) for proteins (2-5 nm thick)
Anti-DNP Mabs
Immobilized DNP-HSA complexes
IR beam

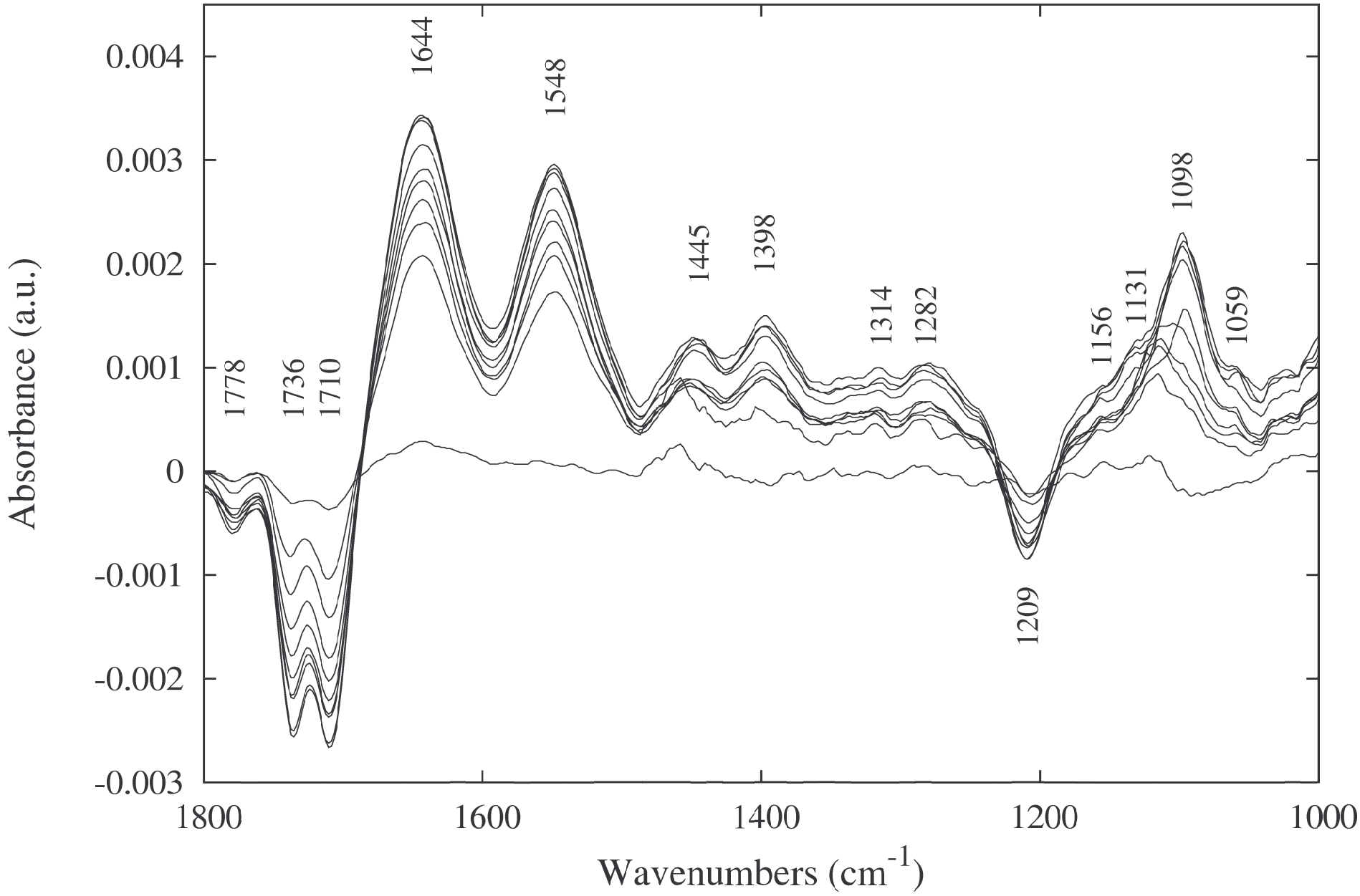
0.004
0.003
0.002
0.001
0
-0.001
-0.002
-0.003
Absorbance (a.u.)
1800
1600
1400
1200
1000
Wavenumbers (cm-1)
1778
1736
1710
1644
1548
1445
1398
1314
1282
1209
1156
1131
1098
1059

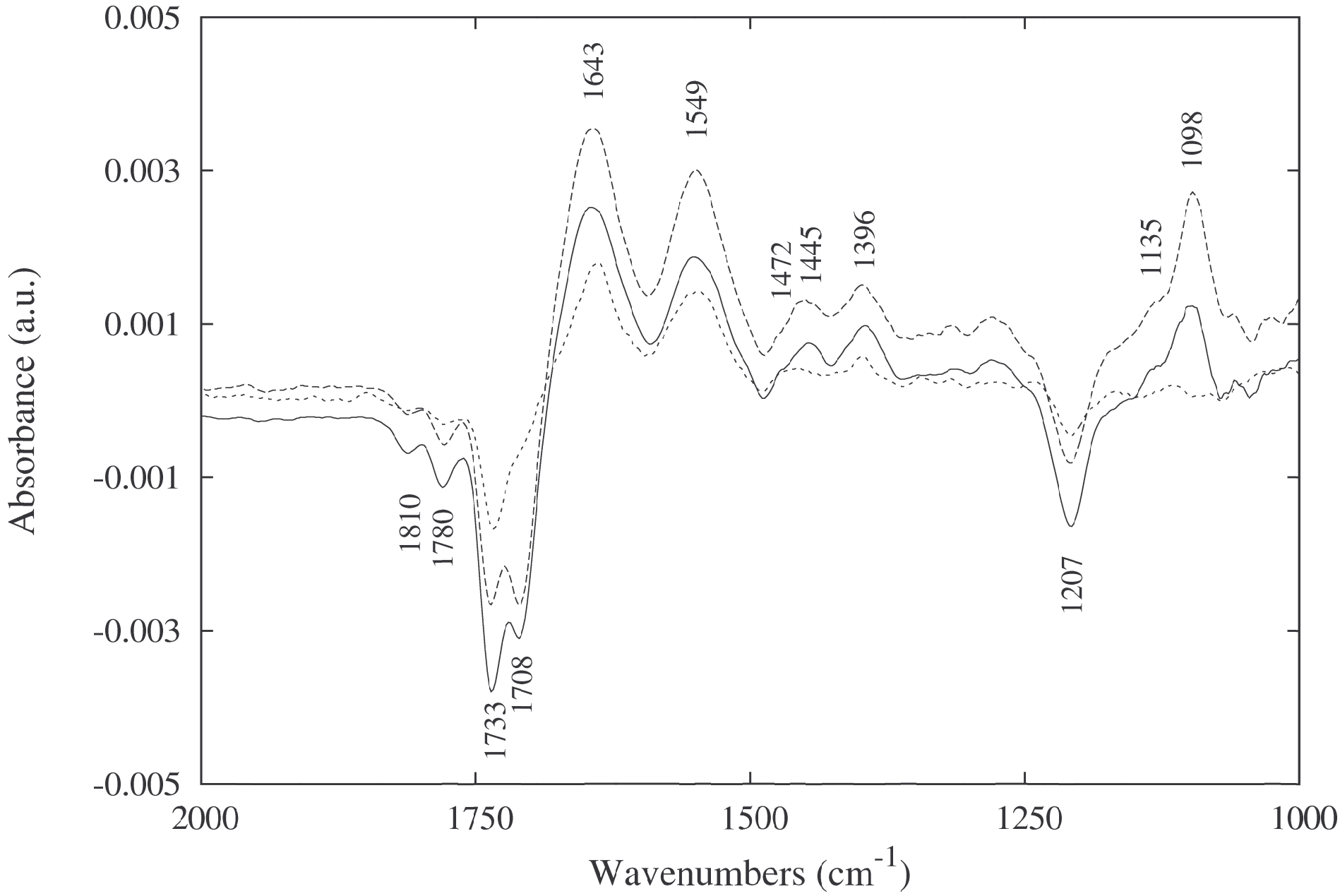
0.005
0.003
0.001
-0.001
-0.003
-0.005
Absorbance (a.u.)
2000
1750
1500
1250
1000
Wavenumbers (cm-1)
1643
1549
1472
1445
1396
1135
1098
1810
1780
1733
1708
1207

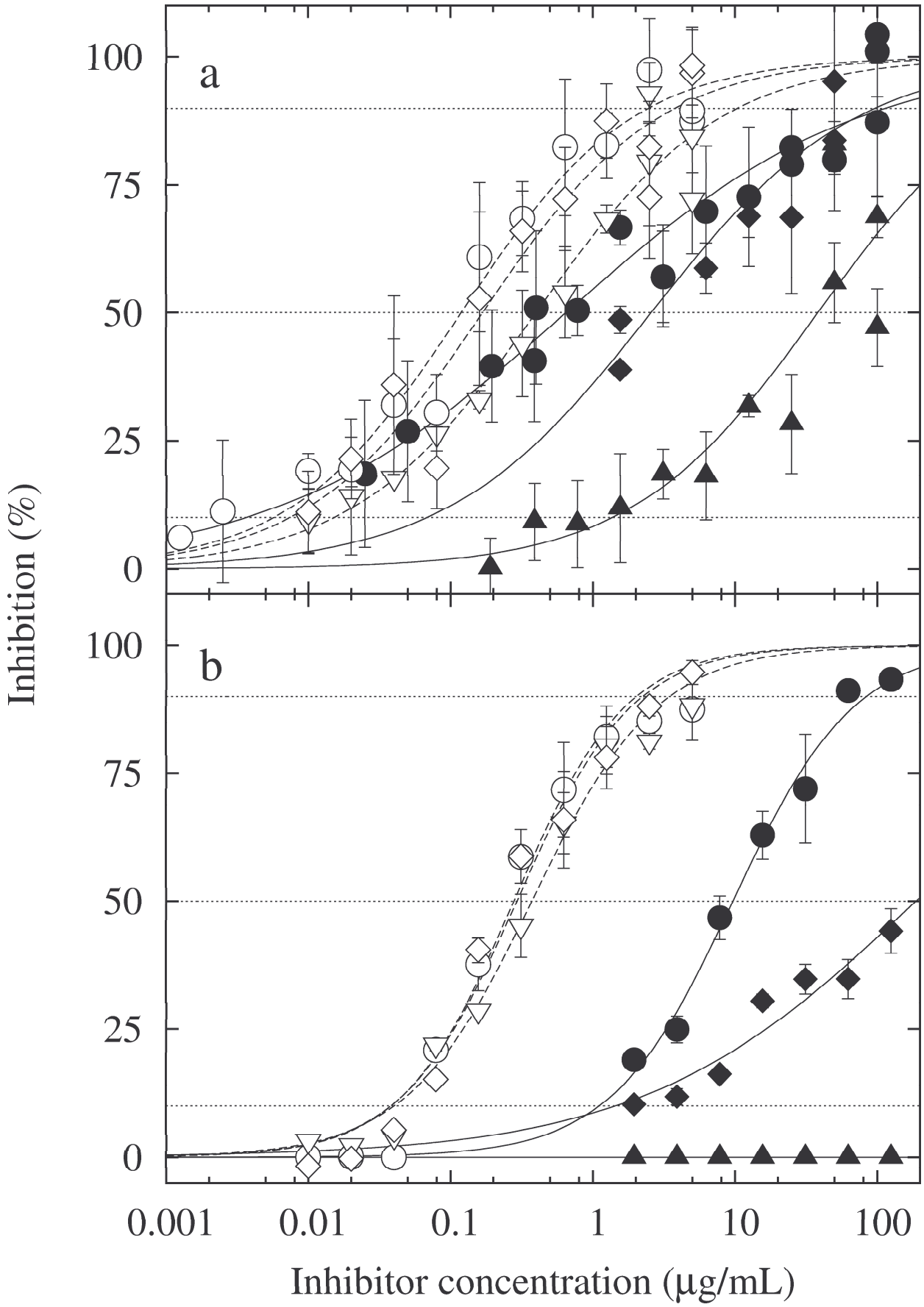
a
b
100
75
50
25
0
Inhibition (%)
0.001
0.01
0.1
1
10
100
Inhibitor concentration (µg/mL)

## Fourier transform infrared immunosensors.

E. Gosselin [a], M. Gorez [a], M. Voué [a,*], O. Denis [b], J. Conti [a], N. Popovic [c], A. Van Cauwenberge [c], E. Noel [c], J. De Coninck [a]

[(a)] CRMM, Université de Mons-Hainaut, Place du Parc, 20, B-7000 Mons (Belgium), [(b)] Instituut Pasteur, WIV, Allergology Unit, Engelandstraat 642, B-1180 Brussels (Belgium), [(c)] Hainaut Vigilance Sanitaire, Boulevard Sainctelette, 55, B-7000 Mons (Belgium)

### Supporting information

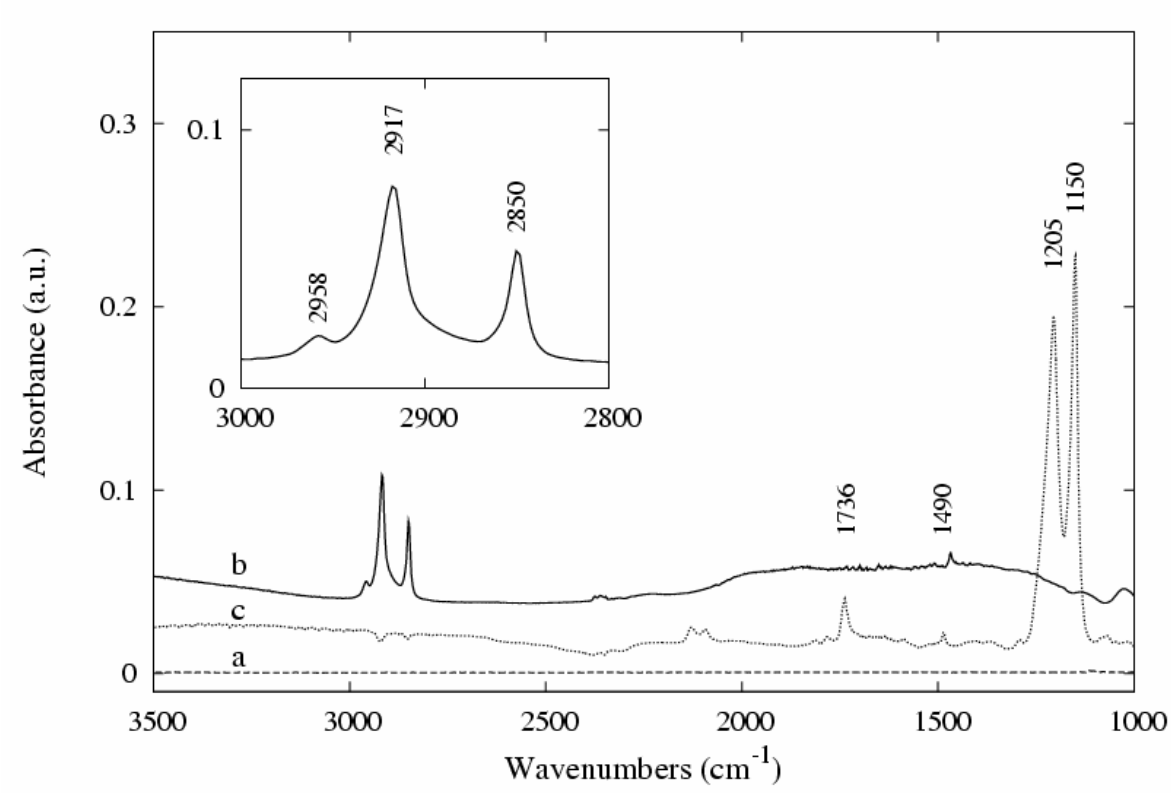


**Figure A1:** FTIR spectra relevant for the layer-by-layer construction of the sensor [a: activated crystal used as baseline – dashed line, b: crystal with OTS layer – plain line, c: crystal with photo-irradiated OTS layer and SADP molecule – dotted line]. Inset: Details of the OTS spectrum in the 3000-2800 cm-1 C-H stretching spectral region.

* Corresponding author. Fax: + 32 65 373881 - Email address: michel.voue@crmm.umh.ac.be (M. Voué).

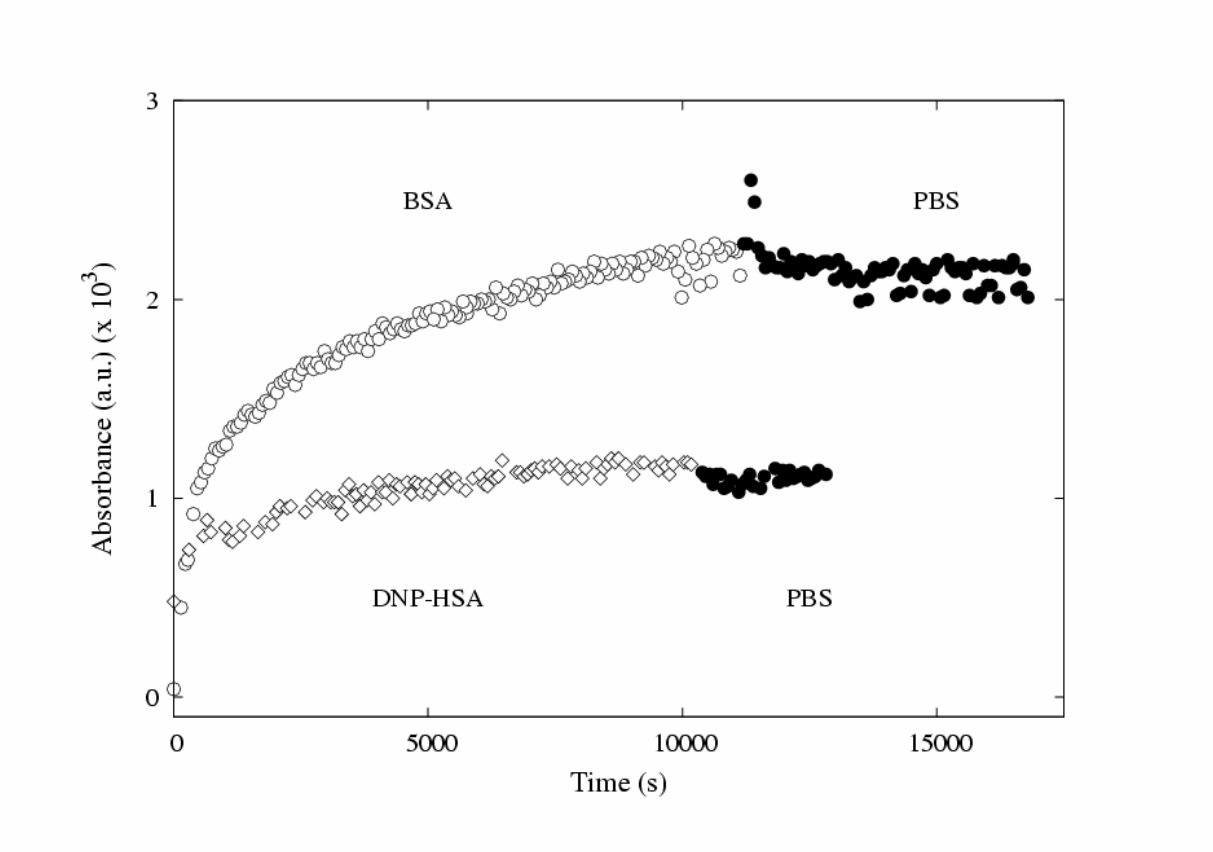


**Figure A2:** Time evolution of the intensity of the Amide II band (1552 cm-1) for the DNP-HSA (open diamonds) and for HSA (open circles). (Filled circles: rinsing by PBS solution, in both cases).

We report hereafter the experimental results concerning the saturation of the unreacted sites of the sensor as well as those concerning the specificity of the molecular recognition.

*a) Saturation of the unreacted site.* After the binding of the coupled protein to the sensor and the rinsing step with PBS solution, a solution of glycine 0.33M (pH 7.2) was injected in the flow cell. The interaction of glycine with the possible unreacted SADP molecules was monitored at 1332 and 1411 $cm^{-1}$. By comparison with the FTIR spectrum of concentrated glycine, we found that these absorption bands were characteristics of the glycine molecules and do not interfere with the amide bands of the protein (data not shown). As, after the glycine pulse, the intensity of the absorption bands comes back to the level of the baseline (Fig. A3a), it can be concluded that the sensor surface is covered at more than 95% by the initially bound protein. This figure also shows the reproducibility of our experiments.

*b) Specificity of the molecular recognition.* In another set of control experiments, the specificity of the molecular recognition of the anti-DNP Mabs was probed by initially binding avidine on the sensor surface, instead of DNP-HSA. The absorbance of the amide II band of the avidine molecules rapidly rises and stabilizes after 5000 s (Fig. A3b). The subsequent pulses of Mabs and of protein-free PBS do not significantly modify its value, confirming the specificity of the antibodies and the stability of the protein layer.

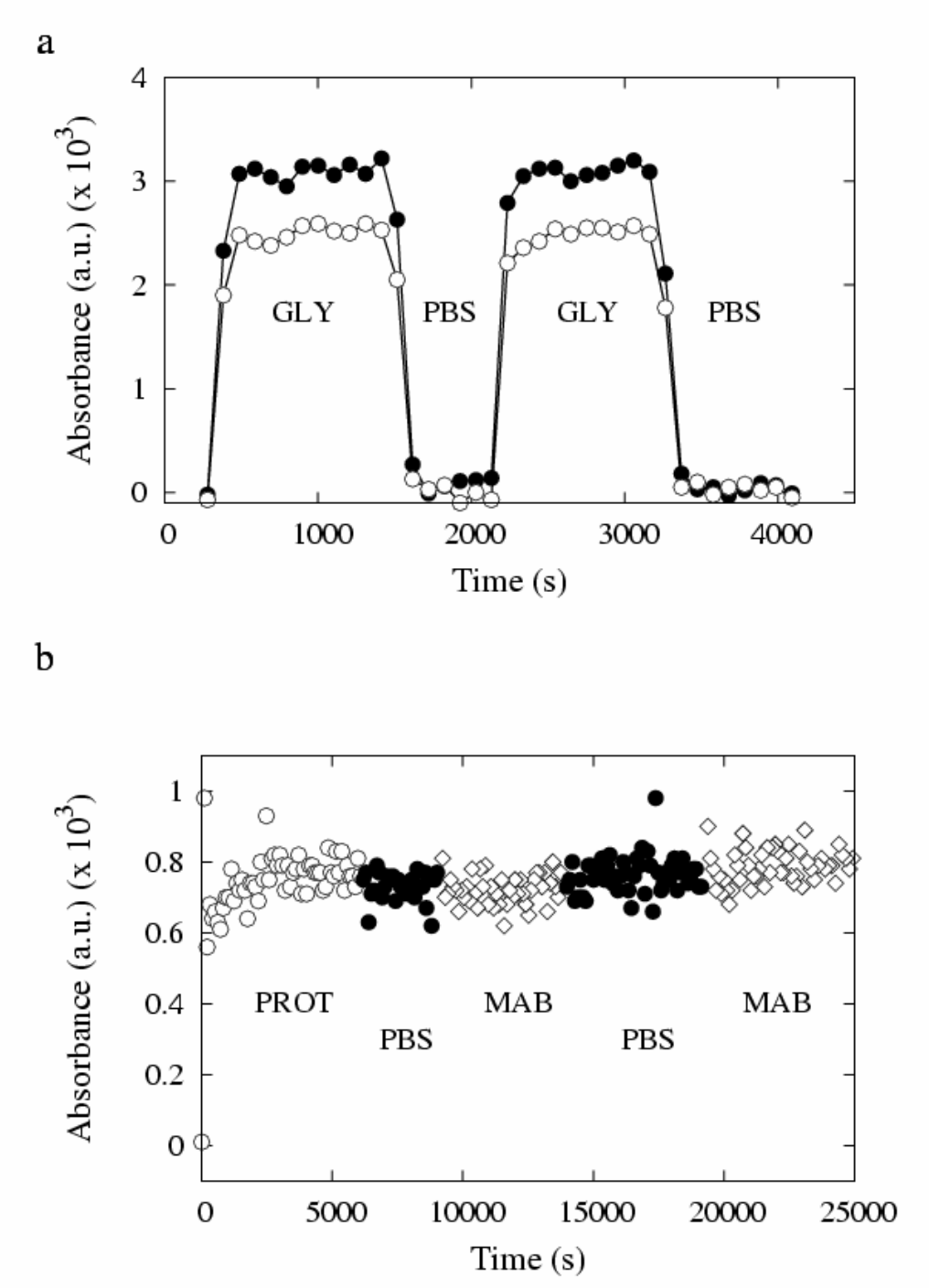

**Figure A3:** (a) Saturation of the unreacted anchoring sites by 0.33 M glycine solution (pH 7.2), as monitored by the specific absorption bands at 1332 $cm^{-1}$ (open circles) and 1411 $cm^{-1}$ (filled circles) of glycine. Sequence of glycine (GLY) and buffer (PBS) pulses. (b) Control for specificity of the molecular recognition of the anti-DNP LO-DNP61 Mab. Flown solutions are the following: avidine 1 mg/ml (PROT – open circles), rinsing buffer (PBS – filled circles), anti-DNP LO-DNP61 monoclonal antibody (MAB – open diamonds), rinsing buffer (PBS – filled circles) and anti-DNP LO-DNP61 monoclonal antibody (MAB – open diamonds).

# DETECTION OF SMALL MOLECULES IN COMPETITIVE IMMUNOREACTIONS MONITORED BY BIA-ATR SENSORS.

**E. Gosselin [1], M. Gorez [1], M. Voué [1,*], O. Denis [2], J. Conti [1], A. Van Cauwenberge [3], E. Noel [3], J. De Coninck [1]**

[1] CRMM - Université de Mons-Hainaut - Place du Parc, 20 - B-7000 Mons, Belgium
[2] Instituut Pasteur, WIV, Allergology Unit, Engelandstraat 642, B-1180 Brussels, Belgium
[3] Hainaut Vigilance Sanitaire, Boulevard Sainctelette, 55, B-7000 Mons, Belgium

*Corresponding author: M. Voué, Phone: +32 65 373885, Fax: + 32 65 373881, michel.voue@crmm.umh.ac.be

**Abstract:** We report experimental results concerning the detection of 2,4-dinitrophenol, under its free form or coupled to human serum albumin using Fourier Transform Infrared spectroscopy based sensors. Competitive immunoreactions were carried out using several anti-dinitrophenol monoclonal antibodies. Comparison with enzyme-linked immunosorbent assays in competition is given for standard operating conditions. FTIR detection limits are comparable to those obtained by ELISA and the limits of detection is about 10 ng/mL and 1 ng/mL for the free and coupled DNP respectively.

**Keywords:** label-free detection, FTIR, immunoassays

## INTRODUCTION

Sensors based on the molecular recognition of bio-molecules have already attracted intensive interest in many different fields such as medical diagnostics and control, environmental analysis, monitoring of biotechnological processes and quality control in food industry [1]. In a recent article [2], we reviewed some specific aspects of biodetection devices and described a new type of generic biosensors suitable for the investigation of ligand-receptor interactions. These devices were based on the high sensitivity of Fourier transform infrared (FTIR) spectroscopy. This original method was based on the grafting of bifunctional spacer molecules directly at the surface of the germanium ATR element (Fig. 1), avoiding the deposition of an intermediate metal layer [3] or of an inorganic layer by sol-gel technique.

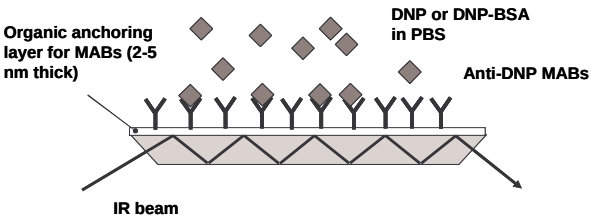


*Figure 1. BIA-ATR biosensors for immunodetection of DNP or DNP-BSA conjugates.*

Such sensors provide spectroscopic information concerning the chemical nature of the interacting molecules, as well as quantitative information concerning the amount of bound receptors and ligands. Furthermore, possible conformational transitions of the receptor during the interaction with its ligand can also be monitored. This information is usually not accessible using standard sensors such as surface plasmon resonance (SPR) sensors or quartz crystal microbalance (QCM) devices, which only measure the mass loading of the sensor. FTIR based sensors are true label-free sensors because, as the chemical structure of the interacting molecules is directly probed, the technology may be considered as auto-labeled. As previously shown [1,4], the method is suitable for the detection of low-molecular weight molecules.In this article, we consider the detection of 2,4-dinitrophenol (DNP, Fig. 2). This molecule was considered as a model from hapten detection, but could also be used as a test molecule for explosive materials such as 2,4,6-trinitrotoluene (TNT) [5].

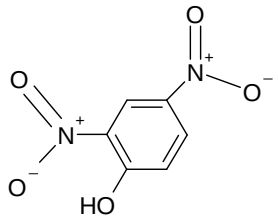


*Figure 2. 2,4-dinitrophenol (DNP)*

## MATERIALS AND METHODS

Unless otherwise stated, the purchased chemicals are of analytical grade and were used as received, without further purification. Anti-DNP monoclonal antibodies were purchased from IMEX (Belgium). The isotypes of the LO-DNP-1, LO-DNP-34 and LO-DNP-61 anti-DNP monoclonal antibodies are respectively: IgG1 kappa, IgM kappa and IgG2a kappa. DNP and DNP-HSA were purchased from Sigma-Aldrich. For the latter molecule, the coupling ratio was 30-40/1, according the manufacturer's information. Phosphate buffer saline solution (PBS) solution was purchased from Sigma-Aldrich.

**FTIR biosensors.** The FTIR biosensors were prepared according to the procedure described by Voué and co-workers [1]. The main steps of the infrared element cleaning and functionalization are summarized hereafter. The internal reflection

elements were silicon ATR prisms (ACM, Villiers St Frédéric, France) with an aperture angle of 45°. Silicon crystals were degreased in chloroform (2 x 5 min) under sonication. Each face of the crystal was exposed to UV radiation in a UV-ozone cleaner (PR100, UVP, England) during 10 min to remove the surface organic contaminants. The crystals were activated in a mixture of $H_2O_2$ – $H_2SO_4$ (7:3 v:v) during 8 min at 150°C before being abundantly rinsed in MilliQ water and dried under a $N_2$ flux. Final activation was carried out in a UV-Ozone cleaner during 15 min. The activated ATR elements were hydrophobized by grafting an octadecyltrichlorosilane (OTS, Sigma-Aldrich) self-assembled monolayer: the activated ATR elements were immersed in a solution of OTS (0.08% v:v) in a mixture of hexadecane and $CCl_4$ (ratio 7:3 v:v) for 16 h at 12 °C [6,7]. The grafted elements were rinsed in chloroform (2 x 5min) under sonication. To avoid dewetting of the spacer molecules solution (see infra), the OTS-grafted surfaces were placed 2 min in a UV-ozone oven (PR100, UVP, UK) at a distance of 5 cm from the UV source. This results in a partial burning of the SAM and of an increase of ATR element critical surface tension. Contrarily to our previous articles [1], commercial spacer molecules were used. N-Succinimidyl (4-azidophenyl) 1,3´-dithiopropionate molecules (SADP, Pierce, USA) were dissolved in acetonitrile (1.8 mg/mL). The SADP solution is sprayed on the partial-OTS surfaces. The solvent was evaporated in the dark before irradiation during 2 hrs at 7 cm of a UV lamp ($\lambda_{max}$ = 254 nm). Photo-grafted surfaces were rinsed in acetonitrile (2 x 5 min) under sonication. The so-obtained surfaces were stable when kept in closed vials at normal storage conditions.

**FTIR experiments.** ATR-FTIR spectra were recorded on a Nicolet 6700 FTIR spectrophotometer (Thermo Electron Corporation, USA) equipped with a liquid $N_2$ cooled MCT detector at a resolution of 2 $cm^{-1}$ with a mirror speed of 0.6329 cm/s. The spectrometer was continuously purged with dry air (Parker-Zander, Germany) at a flow of 30 SCFH. The processing of the spectra was done using the OMNIC 7.3 software (Thermo Electron Corporation, USA). The SADP-functionalized surfaces were placed in an ATR flow cell (Specac, UK) connected to a Watson-Marlow 403U/VM2 peristaltic pump (Farmount, UK). Typical flow speed was 20 µL/min.

**Inhibition tests.** In a first step, a DNP-HSA solution (1 mg/mL in PBS) was injected in the flow cell at a flow rate of 5 µL/min (discontinuous). After 2 h, buffer solution was injected in the cell to remove the unreacted excess of protein. After the binding of the protein to the sensor surface, monoclonal antibodies (Mabs) (5 µg/mL in PBS) were incubated in the presence of either free or coupled DNP. After 20 min of incubation, an aliquot of the Mabs/inhibitor solution was injected in the flow cell and the binding of the antibody to the immobilized protein was monitored as a function of time by recording FTIR spectra.

## RESULTS AND DISCUSSION

**Binding of the coupled protein.** Binding of the coupled protein DNP-HSA to the sensor surface can be quantified and monitored on-line from the FTIR intensity of some specific absorption bands. (Fig. 3A). As the coupling between the protein and the surface requires the hydrolysis of the activated ester of the N-succinimidyl group of the SADP molecule, 4 bands are characteristics of the appropriate anchoring of the protein at the sensor surface: the amide I and amide II absorption bands of the protein, respectively labeled ‘a’ and ‘b’ (Fig. 3A) and the stretching bands ν(C=O) and ν(C-O), respectively labeled ‘c’ and ‘d’. Taking a baseline the spectrum recorded on the SADP-functionalized crystal surface, the two former bands appear in positive mode as they correspond to the binding of the protein, while the two latter appear in negative mode as they monitor the hydrolysis of the reactive function of SADP molecules.

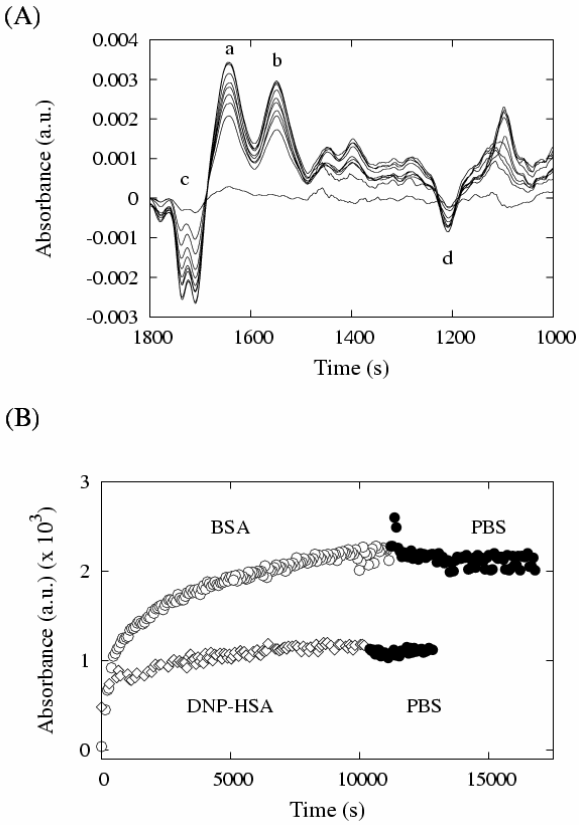


*Figure 3. (A) Time evolution of the FTIR-ATR spectra recorded during the binding of the DNP-HSA molecules on a SADP functionalized silicon crystal. The spectra were recorded every 10 min. (B) Time evolution of the intensity of the Amide II band (1552 $cm^{-1}$) for the DNP-HSA (open diamonds) and for HSA (open circles). (Filled circles: rinsing by PBS solution, in both cases).*

The stability of the anchored protein layer is show in Fig. 3B: the absorbance of the amide II band

remains constant during rinsing of the flow cell with PBS solution. The coupling of DNP to HSA molecules occurs at the level of their peripherical $NH_2$ groups (i.e. mainly on the LYS amino-acids). They are therefore less numerous than in native albumin molecules and the amount of DNP-HSA bound to the sensor surface is less than the one of BSA (Fig. 3B).

**Saturation of the sensor surface by bound proteins.** A series of control experiments were carried out the check the saturation of the binding sites of the sensor. After the binding of the coupled protein to the sensor and the rinsing step with PBS solution, a solution of glycine 0.33M (pH 7.2) was injected in the flow cell. The interaction of glycine with the possible unreacted SADP molecules was monitored at 1332 and 1411 $cm^{-1}$.

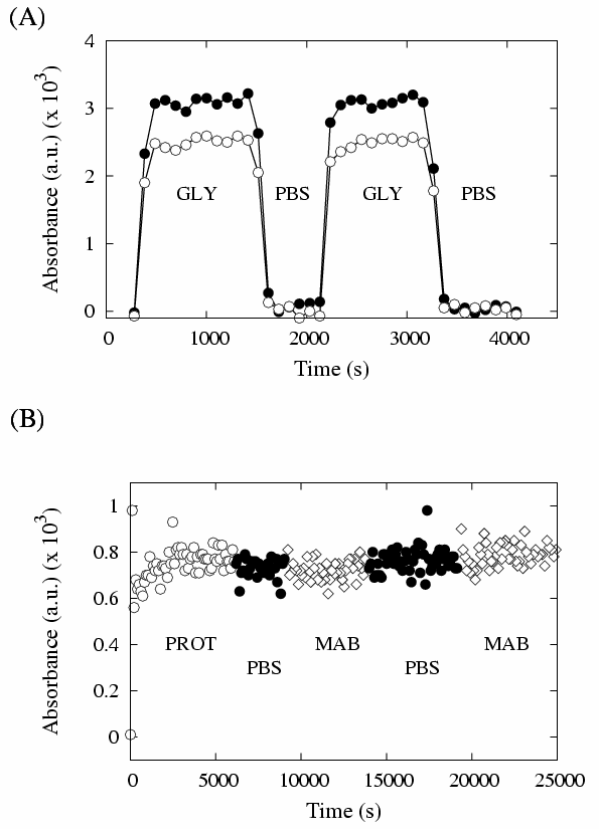


*Figure 4. (A) Saturation of the unreacted anchoring sites by 0.33 M glycine solution (pH 7.2), as monitored by the specific absorption bands at 1332 $cm^{-1}$ (open circles) and 1411 $cm^{-1}$ (filled circles) of glycine. Sequence of glycine (GLY) and buffer (PBS) pulses. (B) Control for specificity of the molecular recognition of the anti-DNP LO-DNP61 Mab. Flown solutions are the following: avidine 1 mg/mL (PROT – open circles), rinsing buffer (PBS – filled circles), anti-DNP LO-DNP61 monoclonal antibody (MAB – open diamonds), rinsing buffer (PBS – filled circles) and anti-DNP LO-DNP61 monoclonal antibody (MAB – open diamonds).*

These absorption bands are characteristics of the glycine molecules and do not interfere with the amide bands of the protein. As, after the glycine pulse, the intensity of the absorption bands comes back to the level of the baseline (Fig. 4A), it can be concluded that the sensor surface is covered at more than 95% by the initially bound protein. This figure also shows the reproducibility of our experiments.

In another set of control experiments, the specificity of the molecular recognition of the anti-DNP Mabs was probed by initially binding avidine on the sensor surface. The absorbance of the amide II band of the avidine molecules rapidly rises and stabilizes after 5000 s (Fig. 4B). The subsequent pulses of Mabs and of protein-free PBS do not significantly modify its value, confirming the specificity of the antibodies and the stability of the protein layer.

**Inhibition tests.** A series of inhibition tests were carried out to probe the sensitivity of the detection method with respect to the coupled or to the free DNP. After binding the coupled protein to the sensor surface, solutions containing Mabs and inhibitors were injected in the flow cell after 20 min of incubation at room temperature. The absorbance of the sample is easily converted in percentage of inhibition *I* by

$$I = 100 - 100\frac{A_i - A_0}{A_{\max} - A_0} \qquad (1)$$

where $A_i$ is the absorbance of the sample, $A_0$ is the absorbance measured after the binding of the protein and the subsequent rinsing with PBS and $A_{max}$ the absorbance measured in the absence of inhibitor. In each case, the absorbance refers to the amide II band.

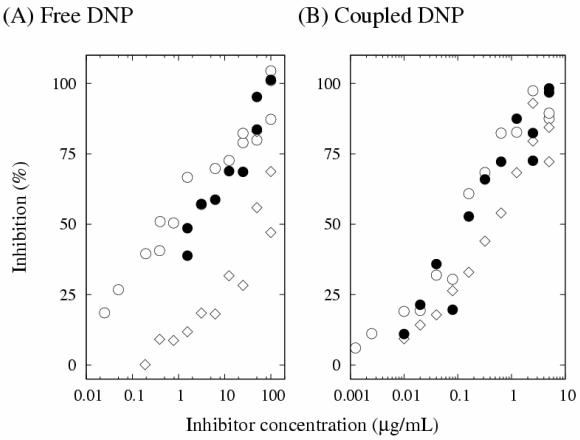


*Figure 5. Inhibition curves for (A) free DNP and (B) coupled DNP. Monoclonal antibodies are LO-DNP61 (open circles), LO-DNP34 (open diamonds) and LO-DNP01 (filled circles).*

Using this experimental scheme, three monoclonal antibodies against DNP were tested: LO-DNP61, LO-DNP34 and LO-DNP01. The results presented in Figure 5 clearly show that these antibodies respond in a different manner to the free or to the coupled molecule. The sensitivity is about 10 times higher for the coupled molecule (Fig. 5B) than for

the free antigen (Fig. 5A). More interesting is the fact that the response of the test also depends on the antibody for the free antigen, although the responses are equivalent for coupled DNP. In the case of free DNP, the LO-DNP34 has sensitivity about 100 times less than the other types of antibodies. Finally, the limit of detection, which can be approximated by the concentration at which 10% of inhibition is reached, is about 10 ng/mL and 1 ng/mL for the free and coupled DNP respectively. Similar results were obtained using ELISA (data not shown).

## CONCLUSIONS

Competitive immunoreactions were carried out using several anti-dinitrophenol monoclonal antibodies and FTIR-ATR based sensors. Two types of inhibitors (free and coupled DNP) were tested. Comparison with enzyme-linked immunosorbent assays in competition is given for standard operating conditions. FTIR detection limits are comparable to those obtained by ELISA and the limits of detection is about 10 ng/mL and 1 ng/mL for the free and coupled DNP respectively.

## REFERENCES


1. S. Andreescu, O.A. Sadik, *Pure Appl. Chem.*, 76 (2004), pp 861-878.
2. M. Voué, E. Goormaghtigh, F. Homble, J. Marchand-Brynaert, J. Conti, S. Devouge, and J. De Coninck. *Langmuir*, 23 (2007), pp 949–955.
3. M. Liley, T.A. Keller, C. Duschl, H. Vogel. *Langmuir* 13 (1997), pp 4190-4192.
4. M. Voué, J. Conti, J. De Coninck, S. Devouge, C. Salvagnini, J. Marchand-Brynaert, F. Homblé, E. Goomaghtigh, *FTIR-ATR biosensors based on a reduced germanium device*, submitted to *Talanta*.
5. H. Aizawa, M. Tozuka, S. Kurosawa, K. Kobayashi, S.M. Reddy, M. Higuchi, *Analytica Chimica Acta*, 591 (2007), pp 191-194.
6. S. Semal, M. Voué, J. Dehuit, M. de Ruijter, J. De Coninck. *J. Phys. Chem. B* 103 (1999), pp 4854–4861.
7. M. Voué, S. Semal, J. De Coninck, *Langmuir* 15 (1999), pp 7855–7862.



(†)This work is supported by the Belgian Scientific Policy (BELSPO) in the framework of the SSD research programme (SD/HE/04A) and by the Ministère de la Région Wallonne. Thanks are due to E. Goormaghtigh, F. Homblé and J. Marchand-Brynaert for helpful discussions.